FORCES ON CYLINDERS OSCILLATING IN WATER

John Robert Driscoll

NAVAL POSTGRADUATE SCHOOL
Monterey, California

THESIS

FORCES ON CYLINDERS OSCILLATING IN WATER

by

John Robert Driscoll, Jr.

Thesis Advisor: C. J. Garrison

December 1972

Approved for public release; distribution unlimited.

Forces on Cylinders
Oscillating in Water

by

John Robert Driscoll, Jr.
Lieutenant, United States Navy
B. S., Saint Joseph's College Philadelphia, 1966

Submitted in partial fulfillment of the
requirements for the degree of

MASTER OF SCIENCE IN MECHANICAL ENGINEERING

from the

NAVAL POSTGRADUATE SCHOOL
December 1972

ABSTRACT

A circular cylinder immersed in an infinite fluid and oscillated perpendicular to its axis is acted upon by a fluid dynamic force. This force is generally considered to be composed of two components, a drag and an added mass component. The relative importance of these are functions of the frequency and displacement of the cylinder.

It was the purpose of this study to determine experimentally these two components as a function of the ratio of the displacement amplitude to the cylinder diameter, and the Reynolds number based on the maximum velocity.

TABLE OF CONTENTS

LIST OF FIGURES

ACKNOWLEDGEMENTS

The author wishes to acknowledge the following members of the Department of Mechanical Engineering Staff, Messieurs J. Beck, G. Baxter and T. Christian for their technical expertise in the construction of the apparatus.

The author gratefully acknowledges the participation of Dr. C. J. Garrison of the Naval Postgraduate School, his advisor, for the constructive supervision and encouragement towards bringing the investigation to fruition.

The author's wife, Jean, has faithfully worked with him throughout. She has been a constant source of encouragement and in so many ways deserves a special Thank-you.

I. INTRODUCTION

With the increased deployment of submerged ocean structures the need to predict the forces exerted on bodies immersed in an oscillating flow is of practical importance. Studies conducted by Reid and Bretschneider [1] on submerged structures stress the necessity of having these forces forecast, given a stated set of wave parameters.

A number of studies have been carried out to determine the values of the added mass and drag coefficient for a pile in ocean waves. Many of these are represented in a correlation of drag coefficient versus Reynolds number presented by Wiegel [2]. However, his plot shows an order of magnitude scatter in the values.

Few basic studies of forces exerted on bodies in oscillating flow have been conducted. Of these, however, the most well known was carried out by Keulegan and Carpenter [3]. They conducted tests with a stationary cylinder placed at the node of a standing wave and obtained a correlation of Cm (mass coefficient) and Cd (drag coefficient) versus Um T/D, where Um denotes the maximum velocity, T the period, and D the cylinder diameter. It was suggested by Keulegan and Carpenter that the parameter, Um T/D, or equivalently, the relative fluid displacement, A/D, was the parameter of primary importance; the effect of Reynolds number was assumed to be of little influence on the values of the drag and added mass coefficients. It is noted, however, that the test method used by Keulegan and Carpenter allowed no control over the Reynolds number so that they had no convenient method of testing this influence.

Heinzer [4] conducted visual studies of an oscillating circular cylinder and concluded that the wake characteristics were primarily dependent upon amplitude of oscillation vice Reynolds number.

Sarpkaya and Garrison [5] investigated unidirectional flow past a cylinder with constant acceleration. Their work lead to the fact that drag and inertial forces are representable as functions of the relative displacement of the fluid. These studies were conducted in the range of Reynolds numbers near 10^4 and no attempt was made to investigate the effect of the Reynolds number.

In the present study various circular cylinders were oscillated with simple harmonic motion in water at rest. Both the amplitude and the frequency of oscillation were controllable so that both the effect of Reynolds number and relative displacement of the fluid could be studied. However, time limitations restricted the experimental program to a series of runs carried out at one fixed Reynolds number with increasing relative displacement. Also, at a fixed value of relative displacement the effect of Reynolds number was determined.

II. METHOD OF APPROACH

This study utilized test cylinders of 4 inches, 2.75 inches and 1.5 inches diameter, 16.5 inches long mounted on a dynamometer. The dynamometer was basically composed of a cantilever beam affixed with strain gauges. The strain gauge bridge error was read out on a strip chart recorder calibrated to read directly in pounds force.

The force traces were read visually at twenty intervals over a complete cycle and this numerical force data used as an input to a data reduction program (Appendix A and B) based on Morison's equation.

Morison et. al. [6] consolidated the three part equation of McNown and Wolf [7].

$$F = Ao\ \rho\ \frac{d(kU)}{dt} + \oint Px\ ds + \frac{1}{2}\ Cd\ D\ \rho\ \ U|U| \qquad (1)$$

by combining the first two terms to yield

$$F = Cm\ \rho\ \ Ao\ \frac{dU}{dt} + \frac{1}{2}\ Cd\ D\ \rho\ \ U|U| \qquad (2)$$

where
F --- Force per Unit Length
Ao --- Circular Cross Section Area of Cylinder
D --- Body Dimension Normal to Flow
ρ --- Density of Fluid
t --- Time
Cd --- Coefficient of Drag
Cm --- Added Mass (Inertia) Coefficient
U --- Velocity at Time t

Equation (2) is assumed valid and is used as the basis of the data reduction.

In the present instance the velocity of the cylinder is represented by:

$$U = -Um \cos \sigma t \tag{3}$$

where Um denotes the maximum velocity, T the period, and $\sigma = 2\pi/T$. The total force acting on the cylinder per unit length is in general given by

$$F = f(t, T, Um, D, \rho, \nu) \tag{4}$$

Grouping the variables on the basis of dimentional reasoning and introducing $\alpha = 2\pi t/T$ gives

$$\frac{F}{Um^2 D} = f(\alpha, \frac{UmT}{D}, \frac{UmD}{\nu}) \tag{5}$$

where $\frac{UmD}{\nu}$ is a Reynolds number and $\frac{UmT}{D}$, which can also be expressed as $\frac{2\pi A}{D}$, will be termed the relative displacement.

Because of flow symmetry and the periodic nature of the force

$$F(\alpha) = -F(\alpha + \pi) \tag{6}$$

it is possible to express the force coefficient in a Fourier series,

$$\begin{aligned}\frac{F}{Um^2 D} = {} & A_1 \sin \alpha + A_3 \sin 3\alpha + A_5 \sin 5\alpha + \dots \\ & + B_1 \cos \alpha + B_3 \cos 3\alpha + B_5 \cos 5\alpha + \dots\end{aligned} \tag{7}$$

where the coefficients A_N, B_N are independent of α and at most functions of Reynolds number and relative displacement. Fourier analysis may be used to determine the coefficients as:

$$A_N = \frac{1}{\pi} \int_0^{2\pi} \frac{F \sin N\alpha}{\rho U m^2 D} \, d\alpha \tag{8}$$

and

$$B_N = \frac{1}{\pi} \int_0^{2\pi} \frac{F \cos N\alpha}{\rho U m^2 D} \, d\alpha \tag{9}$$

Once obtained, the dependence of these coefficients on Reynolds number and relative displacement may be established provided the data are sufficient.

The general formulation, equation (7), may be reconciled with Morison's equation (2). Introducing U from equation (3) into equation (2)

$$\frac{F}{\rho U m^2 D} = \frac{\pi}{4} Cm \cdot \frac{D\sigma}{Um} \sin \alpha - \frac{Cd}{2} \left| \cos \alpha \right| \cos \alpha \tag{10}$$

By the rule of Fourier

$$\left| \cos \alpha \right| \cos \alpha = \sum_{N=0}^{\infty} \int_0^{2\pi} \frac{\left| \cos \alpha \right| \cos \alpha \cos N\alpha d\alpha}{\int_0^{2\pi} \cos^2 N\alpha d\alpha}$$

$$= a_0 + a_1 \cos \alpha + a_2 \cos 2\alpha + a_3 \cos 3\alpha + \ldots$$

where

$$a_{even} = 0, \quad a_{odd} = (-1)^{\frac{N+1}{2}} \frac{8}{N(N^2-4)\pi} \tag{11}$$

The first three non-zero coefficients would then be:

$$a_1 = 8/3\pi, \qquad a_3 = 8/15\pi, \qquad a_5 = 8/105\pi \tag{12}$$

Introducing equation (12) into equation (7) with

$$\begin{aligned} B_1' &= B_1/a_1 \\ B_3' &= B_3 - a_3/a_1 \left(B_1\right) \\ B_5' &= B_5 - a_5/a_1 \left(B_1\right) \end{aligned} \tag{13}$$

yields

$$\begin{aligned} \frac{F}{\rho U m^2 D} &= A_1 \sin \alpha + A_3 \sin 3\alpha + A_5 \sin 5\alpha + \ldots \\ &+ B_1' \left| \cos \alpha \right| \cos \alpha + B_3' \cos 3\alpha + B_5' \cos 5\alpha + \ldots \end{aligned} \tag{14}$$

Equations (14) and (7) may be compared. Writing

$$\frac{\pi}{4} Cm \cdot \frac{D\sigma}{Um} = A_1 + A_3 \frac{\sin 3\alpha}{\sin \alpha} + A_5 \frac{\sin 5\alpha}{\sin \alpha} + \ldots \tag{15}$$

and

$$\frac{Cd}{2} = -B_1' - \frac{B_3' \cos 3\alpha}{\left|\cos \alpha\right| \cos \alpha} - \frac{B_5' \cos \alpha}{\left|\cos \alpha\right| \cos \alpha} + \ldots \tag{16}$$

Thus, if the coefficients A_3, A_5 and B_3', B_5' vanish, the values of Cm and Cd remain constant for all phases of the cylinder motion

$$Cm = \frac{2}{\pi^2} \frac{UmT}{D} A_1 \tag{17}$$

Substituting A_1 from equation (8) yields

$$Cm = \frac{2}{\pi^2} \frac{UmT}{D} \int_0^{2\pi} \frac{F \sin \alpha \, d\alpha}{\rho Um^2 D} \tag{18}$$

$$Cd = -2B_1' \tag{19}$$

substituting from equations (9) and (13) yields

$$Cd = \frac{-3}{4} \int_0^{2\pi} \frac{F \sin \alpha \, d\alpha}{\rho Um^2 D} \tag{20}$$

If the coefficients do vary with the phase α, the values given by equations (18) and (20) are weighted averages. With this possibility in mind it is preferable to adopt

$$\frac{F}{\rho Um^2 D} = A_1 \sin \alpha + B_1' \cos \alpha \, | \cos \alpha | + \text{error} \tag{21}$$

or

$$\frac{F}{\rho Um^2 D} = \frac{\pi}{4} Cm \cdot \frac{D\sigma}{Um} \sin \alpha - \frac{Cd}{2} | \cos \alpha | \cos \alpha + \text{error} \tag{22}$$

where A_1, B_1', Cm and Cd are constant and error has the value

$$\begin{aligned} \text{error} = {} & A_3 \sin 3\alpha + A_5 \sin 5\alpha \\ & + B_3' \cos 3\alpha + B_5' \cos 5\alpha \end{aligned}$$

This error is obtained by subtracting the computed value of $A_1 \sin \alpha$ and $B_1' \, | \cos \alpha | \cos \alpha$ from the observed $F/\rho Um^2 D$.

The foregoing formulation was developed by Keulegan and Carpenter [3] and equations (18), (20) and (22) were the basis for the computer data reduction program developed in Appendix A and presented in Appendix B.

III. APPARATUS

A. TEST BASIN

A test basin, 16 feet long, 4 inches deep, and 16.5 inches wide was constructed from 3/4 inch AC marine plywood. The side walls were supported at approximately 20 inch intervals with 1.5 inch thick plywood gussets and two 2 by 6 inch pine stringers along the top edge of the tank, Figure 1.

The presence of considerable width-tolerance variance when the tank was filled, necessitated the addition of three 2 by 1 inch channel braces, welded in an inverted U-shape, placed over the top of the channel. The brace design allowed for unobstructed motion of the dynamometer along the length of the tank, an advantage not afforded by structural cross braces along the tank top, Figure 2.

All joints were sealed with RTV and inside surfaces were treated with five coats of penetrate and five coats of epoxy paint. Two 3/4 inch thick plexiglass windows, Figure 3, (20 inches by 12 inches) were installed near the tank midsection.

B. DRIVING MECHANISM

The driving mechanism consisted of a "Dynamatic" electric motor with an eddy-current clutch and Mark III controller. This system utilized a closed loop feedback to linearize and stabilize its shaft speed. The basic control system used is presented schematically in Figure 4.

Figure 1: Tank Side Wall Construction

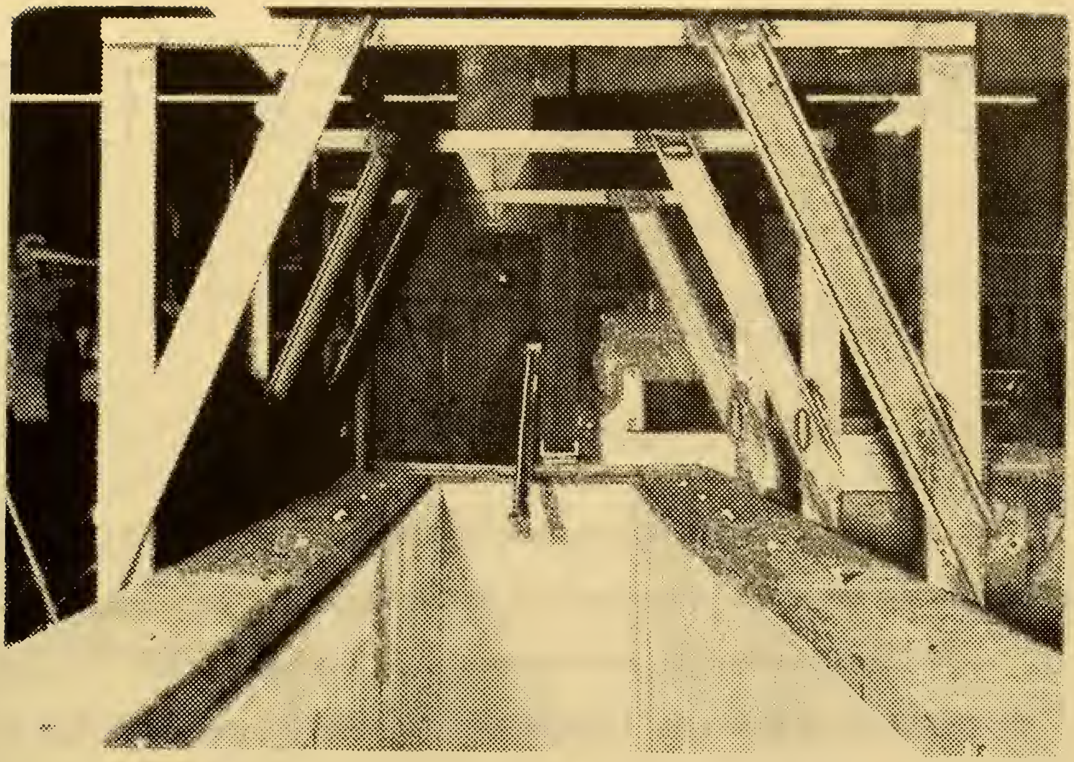

Figure 2: Cross Braces

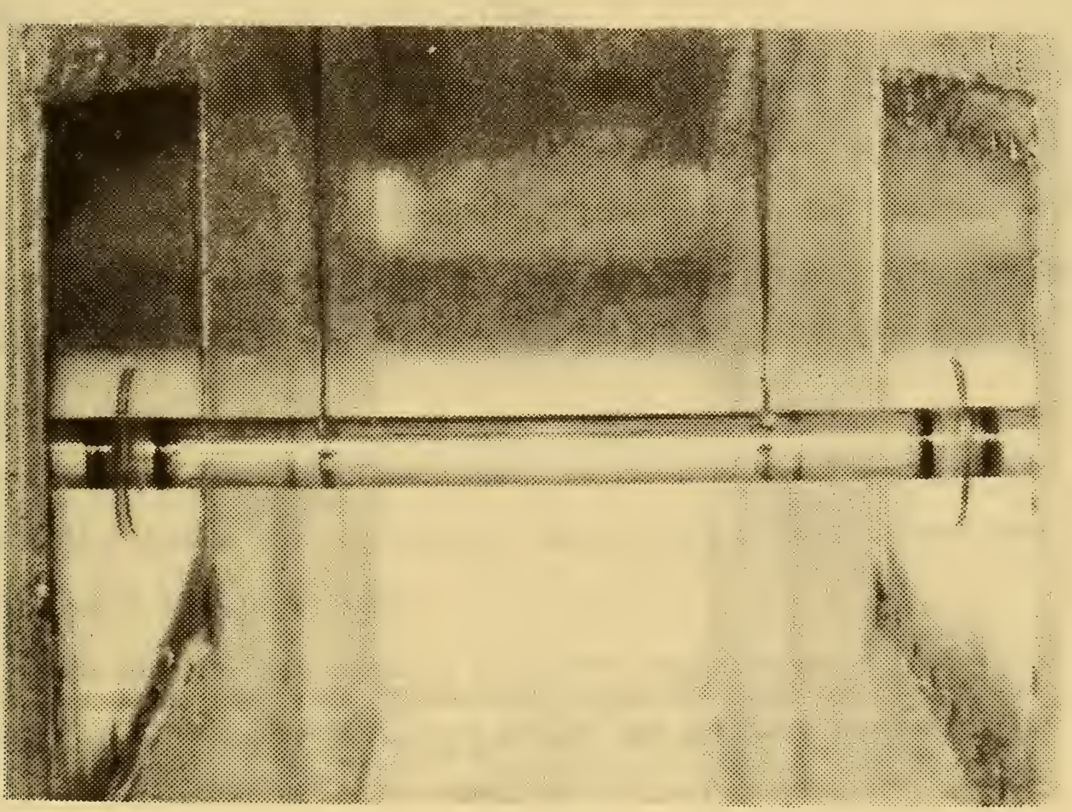

Figure 3: Test Section Windows

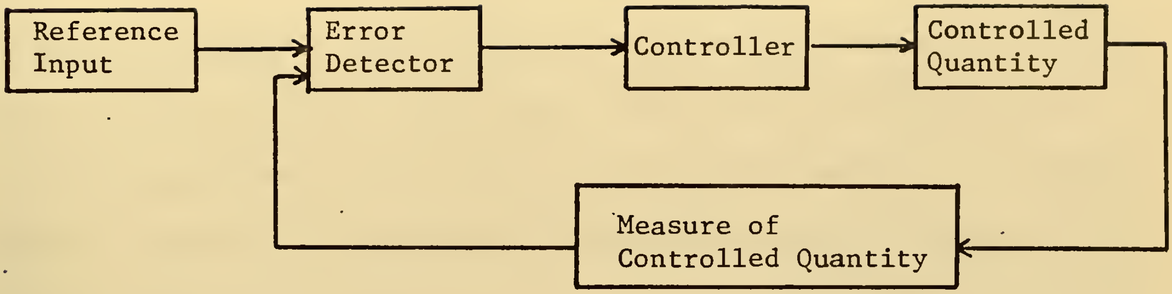

Figure 4: Feedback Loop

More specifically, the controlled quantity is the shaft speed, the reference input is a potentiometer and the error detector is a summing amplifier. The controller is a combination of a power amplifier, motor and eddy-current clutch. The measure of shaft velocity is accomplished by means of a tachometer generator, producing an output voltage proportional to shaft velocity.

The summing amplifier detects differences between the desired speed and actual speed. This difference is fed to the power amplifier which modulates the clutch coil current. If the speed is too low, the coil current is increased, causing the eddy-current clutch to transmit more torque to the load. The result is an acceleration of the shaft to desired speed.

The above speed regulation operates for positive loading only. Since the minimum coil current was zero, negative loads caused free rotation of the output shaft.

Both positive and negative loads were experienced by the output shaft due to the connecting rod's weight and carriage inertia. This lead to uneven output shaft speed, particularly at low RPM, and

necessitated the application of a continuous positive load. This load was supplied through a 3 inch wide 17 inch diameter brake drum, affixed to the face plate, with a 120° leather lined brake shoe riding on it.

The assembled motor, face plate and brake were mounted on a separate platform, Figure 5, to isolate any inherent mechanical vibrations from the tank structure. A 7 foot 8 inch long by 1.5 inch diameter thin walled aluminum tube was then used to connect the driving mechanism to the carriage. This long driving rod produced a near sinusoidal motion of the carriage.

C. CARRIAGE

The carriage as shown in Figure 6 provided a movable mounting platform which was positioned over the test tank.

The carriage consisted of a U-shaped, welded aluminum structure fitted with four 3/4 inch linear bearings located at the ends of the hollow cylindrical side members. The sides of the platform were constructed of two inch aluminum pipe fitted with aluminum bearing blocks at each end. The structural transverse member of the carriage was a 2 by 3 inch aluminum box section welded to the end of each pipe. At the opposite ends of the pipes the bearing blocks were connected by a 3/8 inch diameter transverse shaft to accommodate the vertical struts which supported the cylinder.

The U-shaped platform was mounted through linear bearings on two case hardened 3/4 inch shafts. The shaft ends were supported by two 2 by 6 inch steel channels that transversed the width of the tank. These channels were clamped to the stringers along the top of the side walls.

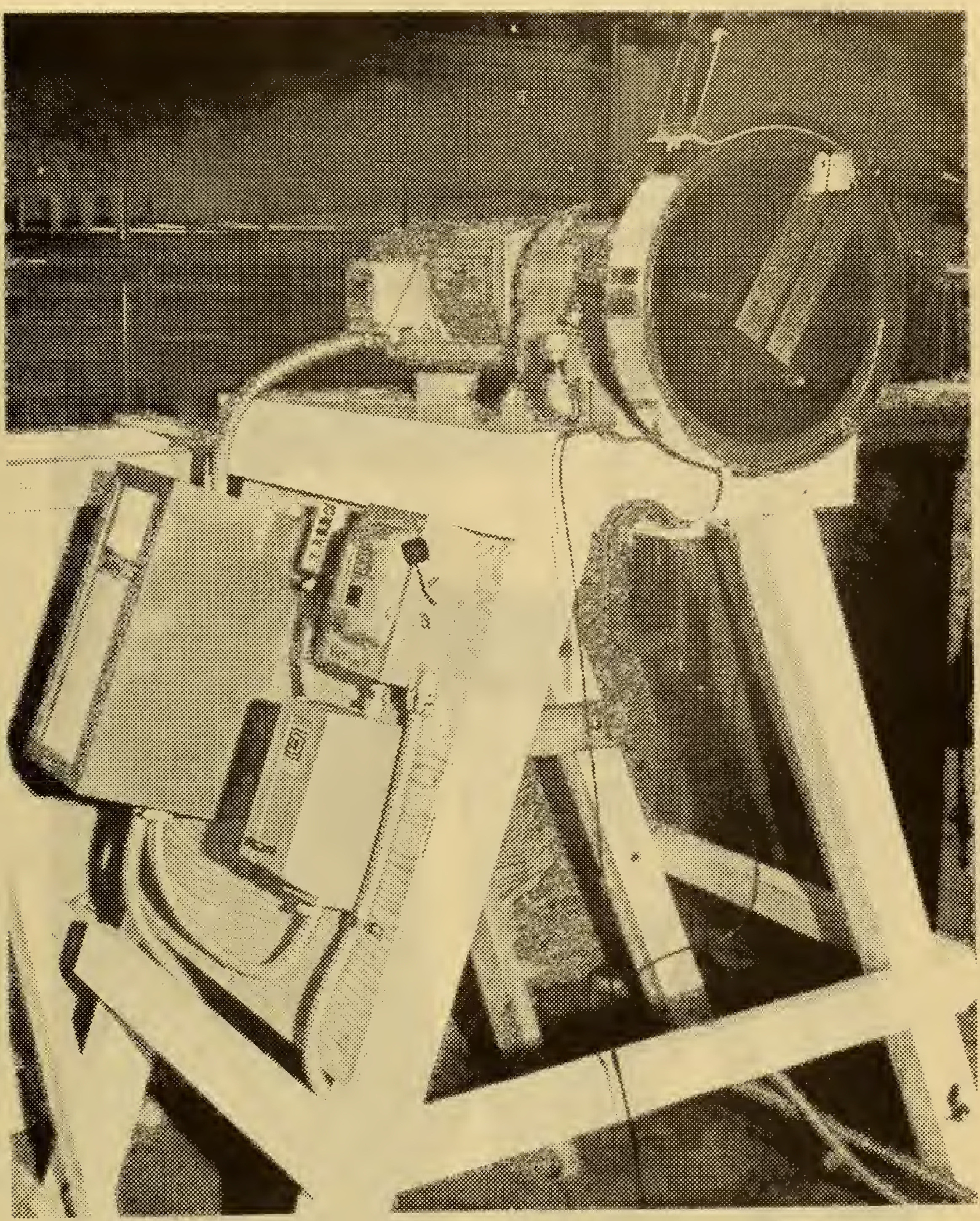

Figure 5: Driving Mechanism

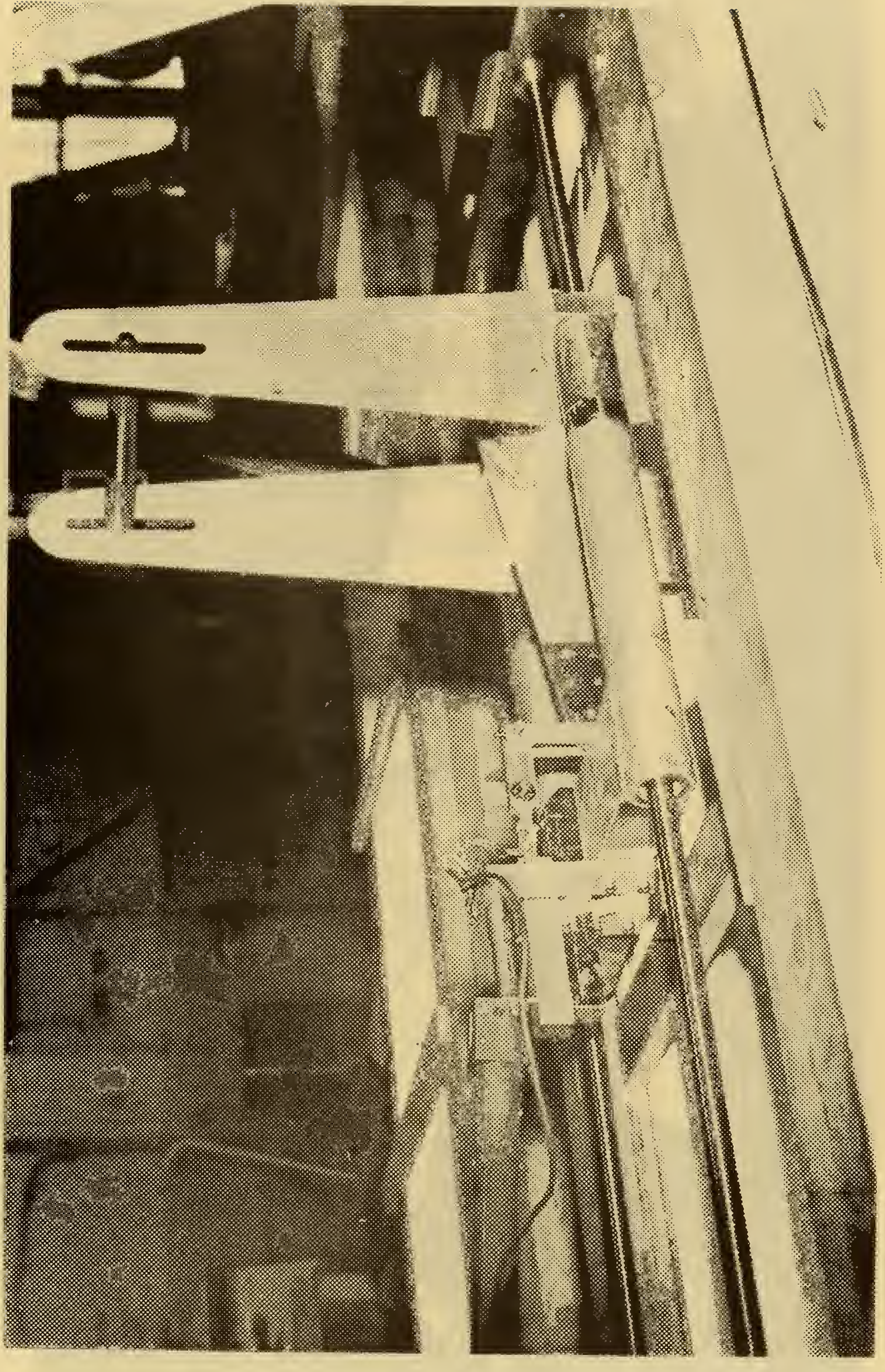

Figure 6: Mounted Carriage Assembly

[illegible]

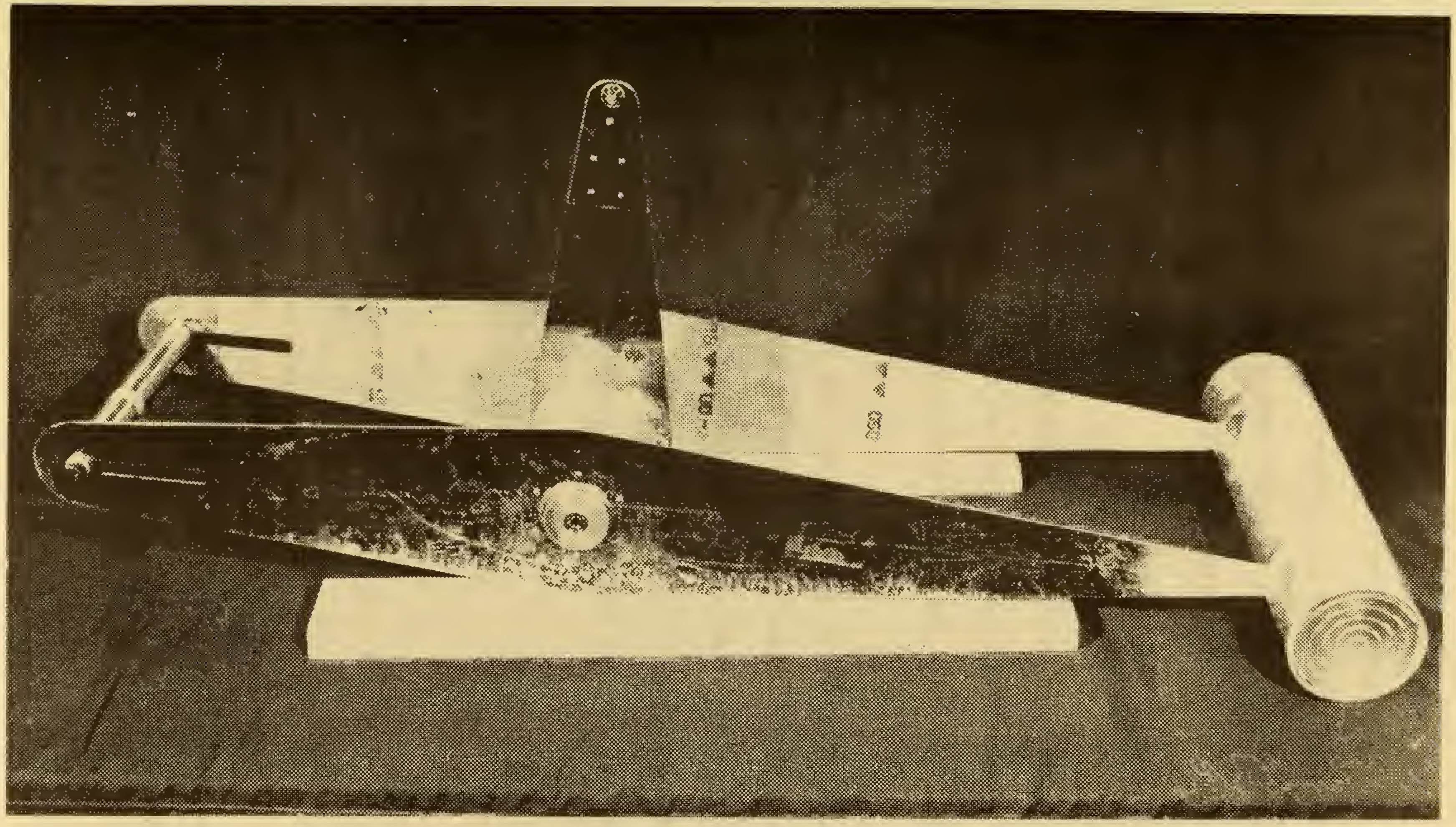

Figure 7: Carriage Cylinder Supporting Arms

The movable part of the carriage consisted of two long arms pivoted near their centers and mounted on a drum as shown in Figure 7. These arms were designed to hold the test cylinders at a maximum centered depth of 18 inches submergence. The leading edges of the tapered 1/16 inch thick polished support arms were sharpened to reduce drag and experimental errors.

A counter balance was placed on the support arms opposite the test cylinder and adjusted so that the center of gravity of the system was at the pivot point. As a result of this balance adjustment the only force (or moment) acting on the arms was due to the fluid; all other inertial loads were balanced out.

A third arm, half the length and perpendicular to the supporting arms, was welded to the center drum. This arm served as a 2:1 mechanical amplifier of force and converted the torque about the rotational center of the drum to a linear force. This force acted, through a pinned ball bearing linkage to a small cantilever beam equipped with strain gages, Figure 8.

D. CANTILEVER BEAMS

Two cantilever beams were constructed, Figure 9;

1. 0.25 inch wide by 0.35 inch high with action arms of 2.5 inch and 4.5 inch
2. 0.6 inch wide by 0.45 inch high with action arms 1.5 inch or 3.5 inch

Two attachment points were provided on each beam so that a large range of forces could be measured without overstressing the beam. Stiffness, and/or sensitivity, could be adjusted to reduce natural frequency vibratory motion by shortening the attachment point or by a change of beams.

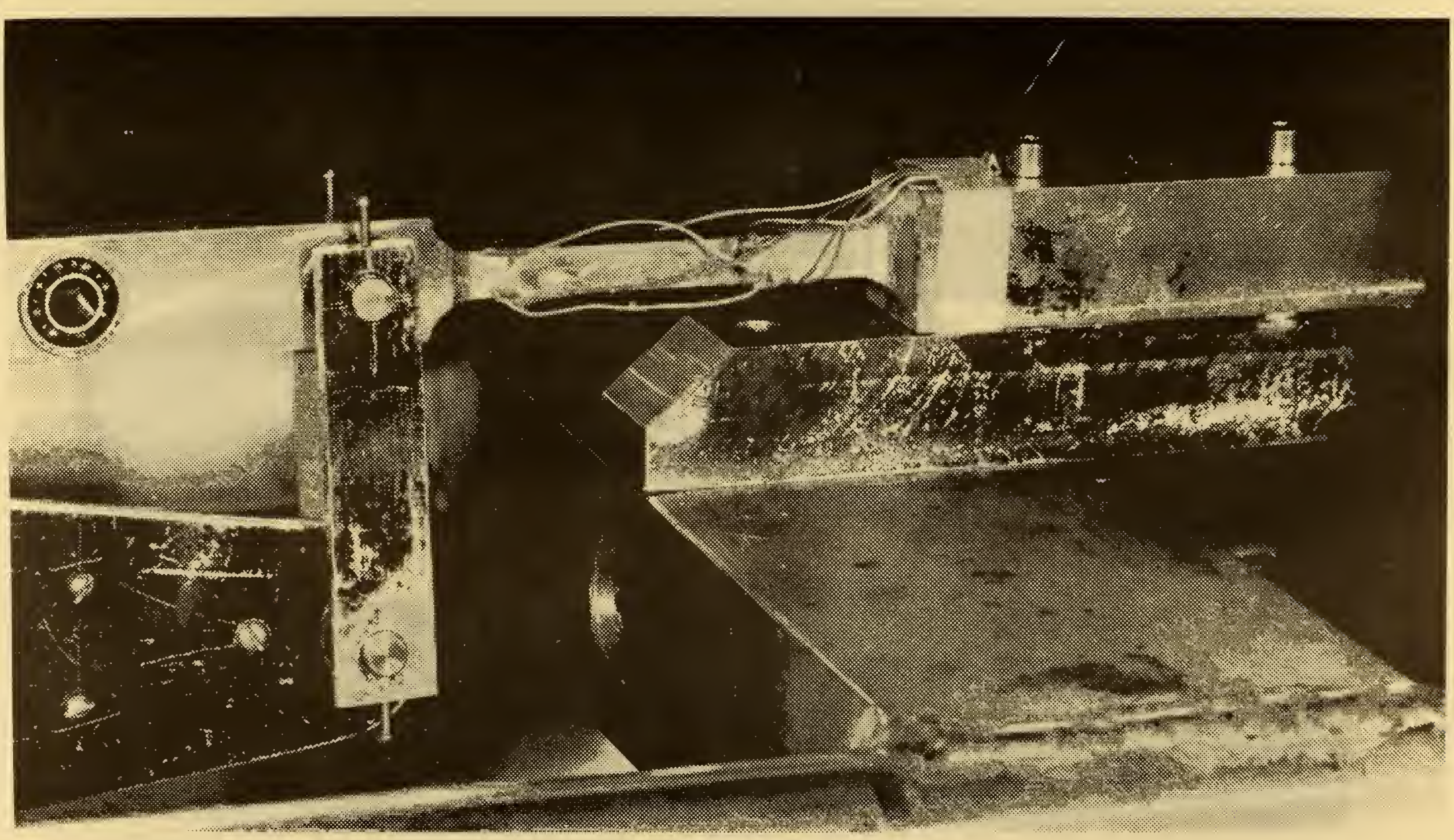

Figure 8: Beam and Link

[illegible]

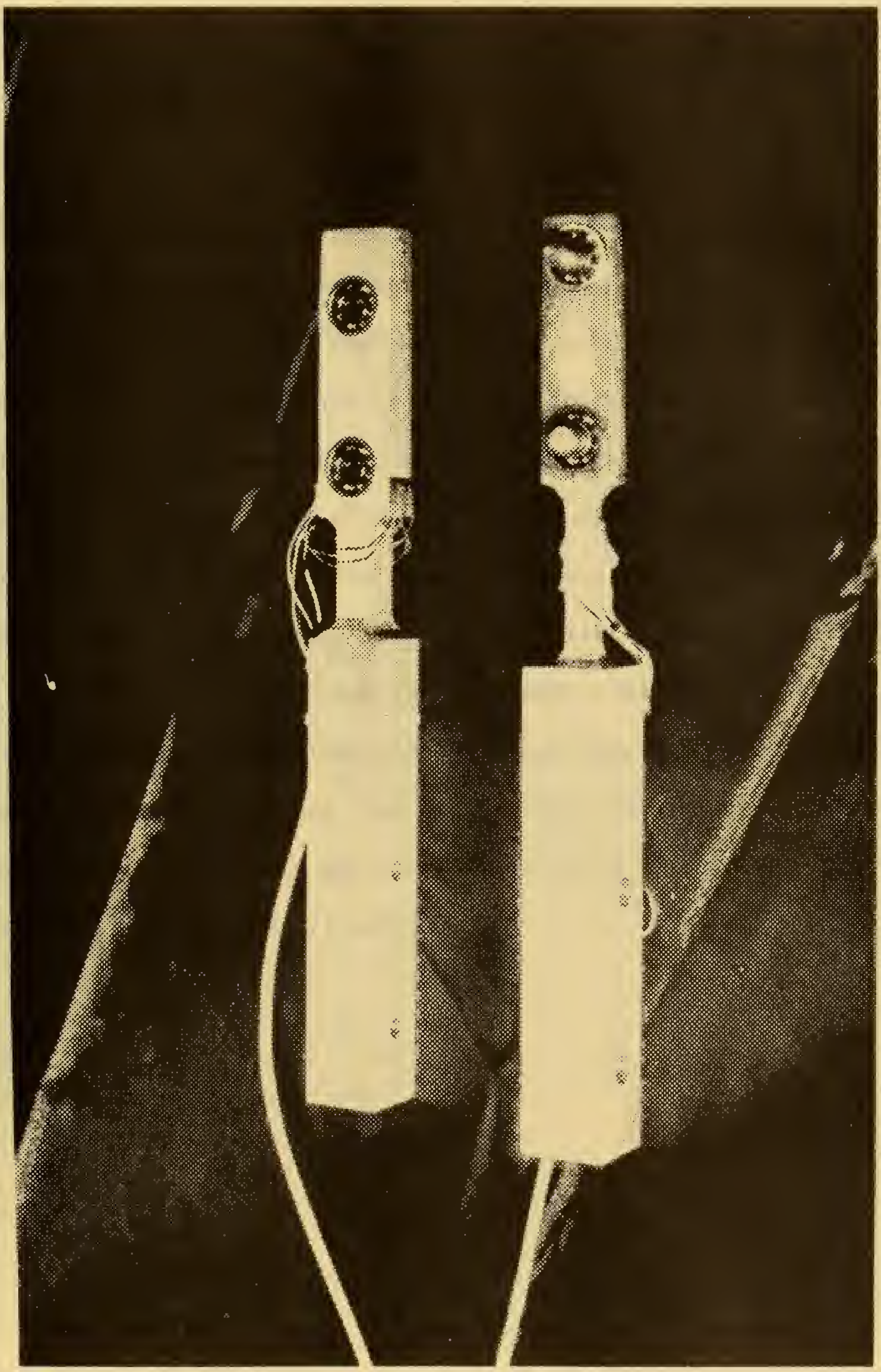

Figure 9: Cantilever Beams

[illegible]

Four strain gauges were applied to each beam to provide a means of measuring forces imposed upon the cylinder and transmitted mechanically through the balance assembly to the beam.

E. TEST CYLINDERS

Three cylinders as shown in Figure 10 were constructed to provide maximum flexibility in testing over a wide range of frequency and displacement. All cylinders were fabricated from plexiglass and slotted to accommodate one end of the vertical support arms. Bulkheads were placed adjacent to the slots to provide attachment points for the ends of the arms. Silicone sealent was used to prevent leakage after the arms were attached. This allowed the cylinder to be unflooded resulting in a minimum fixed mass. End pieces as shown in Figure 11 were also constructed of plexiglass. The ends were fitted into the cylinder with 1/8 inch "O" rings to provide the necessary seal. The outer surfaces of the end pieces had a labyrinth seal cut into the face and 1/16 inch plexiglass end plates, one inch larger than the cylinder. The labyrinth seal and end plates were provided for purposes of reducing the leakage around the ends of the cylinder.

Figure 10: Test Cylinders

Figure 11: Cylinder End Pieces

IV. TEST PROCEDURE

A. SYSTEM SELECTION

Primary consideration was given to the selection of the cantilever beam to be used with each of the test cylinders, trade offs being stiffness and sensitivity. It was concluded that the 4 inch and 2.75 inch diameter cylinders would be run on both beams and the 1.5 inch diameter cylinder tested only on the more sensitive of the two beams. This procedure yielded force traces that could be cross correlated for the 4 inch and 2.75 inch cylinders with the better trace utilized for data.

Once components were selected, they were assembled, balanced, aligned to the tank axis and clamped to the tank edge. The system was then finely balanced in the dynamic mode by adjusting the lever arm of the counter balance weight after observing strip chart traces of high frequency oscillations in air. The counter balance weight was adjusted so that no force was observed when oscillating the carriage in air. The tank was then filled to a level 4 to 6 diameters above the test cylinder and the desired amplitude of oscillation and frequency set. Amplitude settings, i.e., connecting rod eccentricity on the face plate, were in half diameter increments. The frequency setting was either random when observing the Reynolds number parameter or adjusted to maintain a given Reynolds number for studies of the amplitude/diameter parameter.

B. SYSTEM CALIBRATION

1. Force Calibration

A length of fine nicrome wire was attached to the test cylinder, fare lead over a pulley arrangement, attached to the top of the tank.

After a half hour warm up period, the four arm strain gage bridge was electrically balanced in an unloaded state. Then accurate weights were hung from the wire and the resulting deflection of the recorder pen noted. The strain gauge bridge and recorder were calibrated in both the positive and negative direction. The resultant deflections of the recorder pen were accurately plotted against the force imposed, Figure 12. The force calibration proved to be very linear.

This calibration was conducted prior to all test runs.

2. Event Marker Calibration

Timing of the moment of maximum velocity was determined by timing contacts on the drive wheel. The ability of the event marker to record the frequency of the imposed motion and the phase angle between the force and motion was dependent upon the accuracy of the chart speed. However, this speed was checked against internal and external timers and no discrepancy was found.

C. DATA RUN

The system as selected was set in motion and recorder started. To avoid wave reflections from the ends of the tank, the system was oscillated for less than ten cycles and secured. No appreciable standing wave was generated under this procedure and the system was allowed to remain at rest for fifteen minutes before a new data set was initiated. After each data run, the force calibration and event marker position were checked.

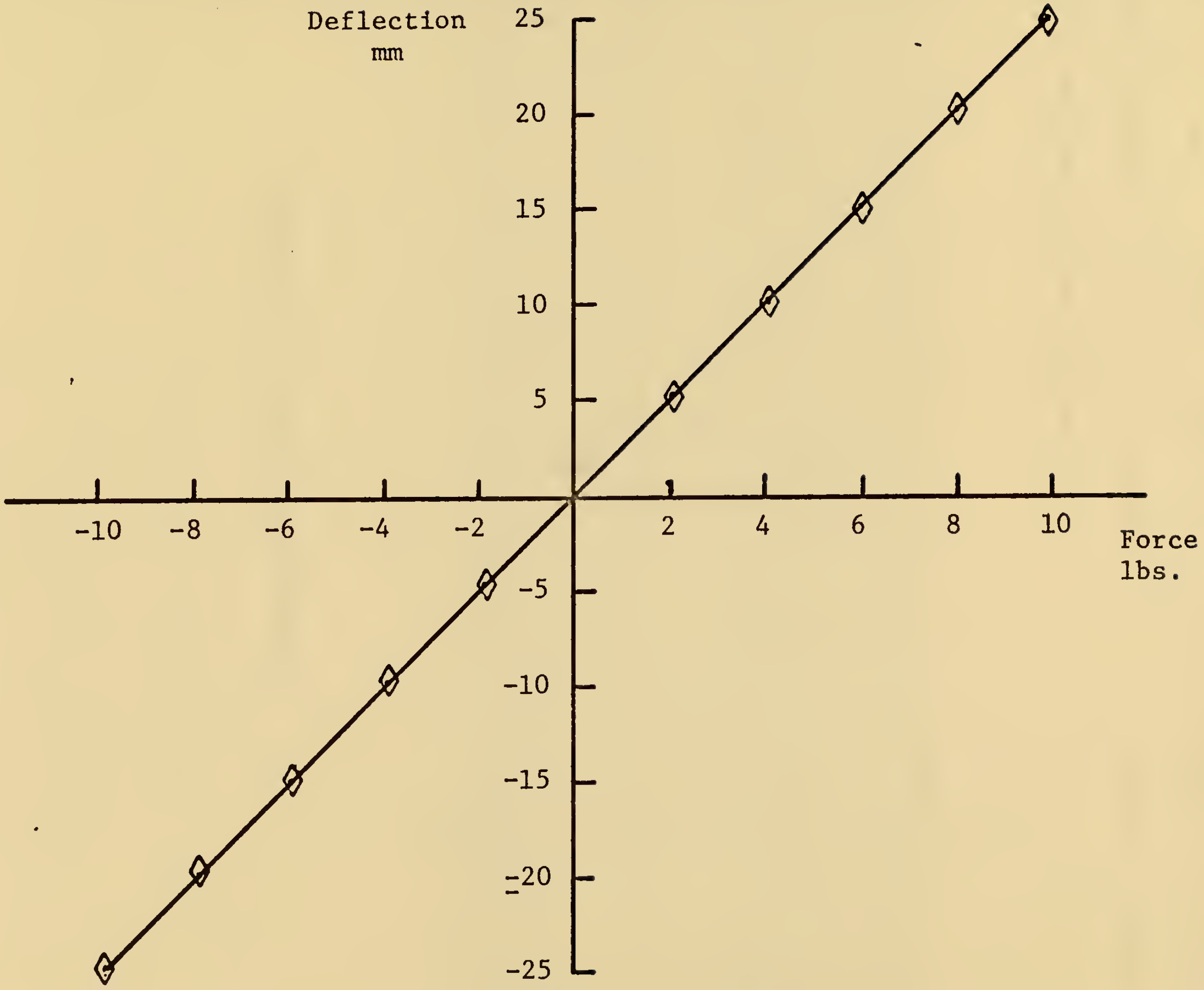

Figure 12: Force Calibration

D. STRIP CHART READ OUT

A mean curve was fared through the force recording to smooth out natural frequency fluctuations and bearing noise. This curve was then divided into twenty divisions, Figure 13, and mid-division force values were read and correlated to its respective t/T for inputs to a data reduction computer program, Appendix B.

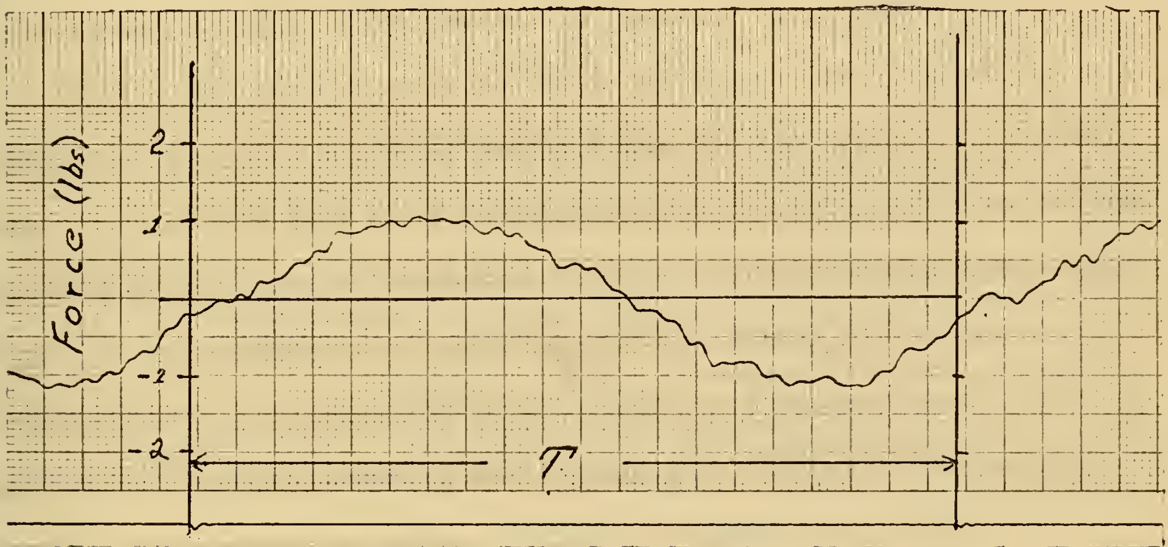

Figure 13: Sample Force Read Out

V. RESULTS

The purpose of the experimental program was to study the effect of the parameter A/D on the added mass and drag coefficients at a fixed Reynolds number. Also a limited number of runs were conducted to determine the effect of Reynolds number on these coefficients at a fixed value of relative displacement, A/D. This latter series of runs was particularly significant since in the past it has been taken for granted that little or no Reynolds number effect occurs in flows of the present type.

Figures 14b and 15b show the total calculated force, based on Figures 14a and 15a, and the observed force for two typical test runs. These figures show that the representation of the total force as the sum of the drag and inertia components is adequate for practical application. Figure 14 corresponds to a case dominated by inertia while Figure 15 corresponds to a larger value of A/D where the drag component is the greatest. The error computed in Appendix A is the difference in the observed and calculated values plotted in Figures 14 and 15.

Figures 16 and 17 show the results for Cd and Cm plotted as a function of A/D for a smooth and rough cylinder. Also, Keulegan and Carpenter's mean value line [3] is plotted for comparison. Keulegan and Carpenter conducted their studies with stationary cylinders and standing waves and, therefore, had no independent means of controlling Reynolds number for a fixed A/D. In general, however, their studies corresponded to fairly low Reynolds number.

It is noted that the mean Cm line taken from their work has been reduced in value by 1.0 to account for differences in test procedure (stationary fluid versus moving fluid).

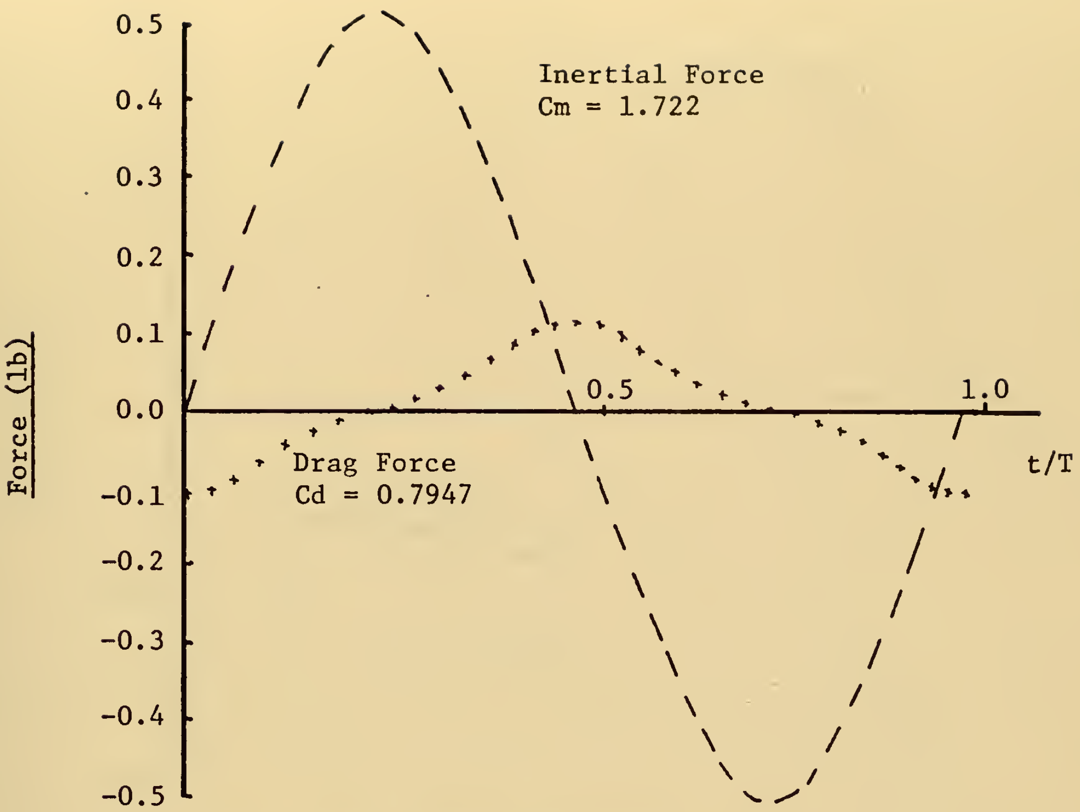

Figure 14a: Drag and Inertial Forces

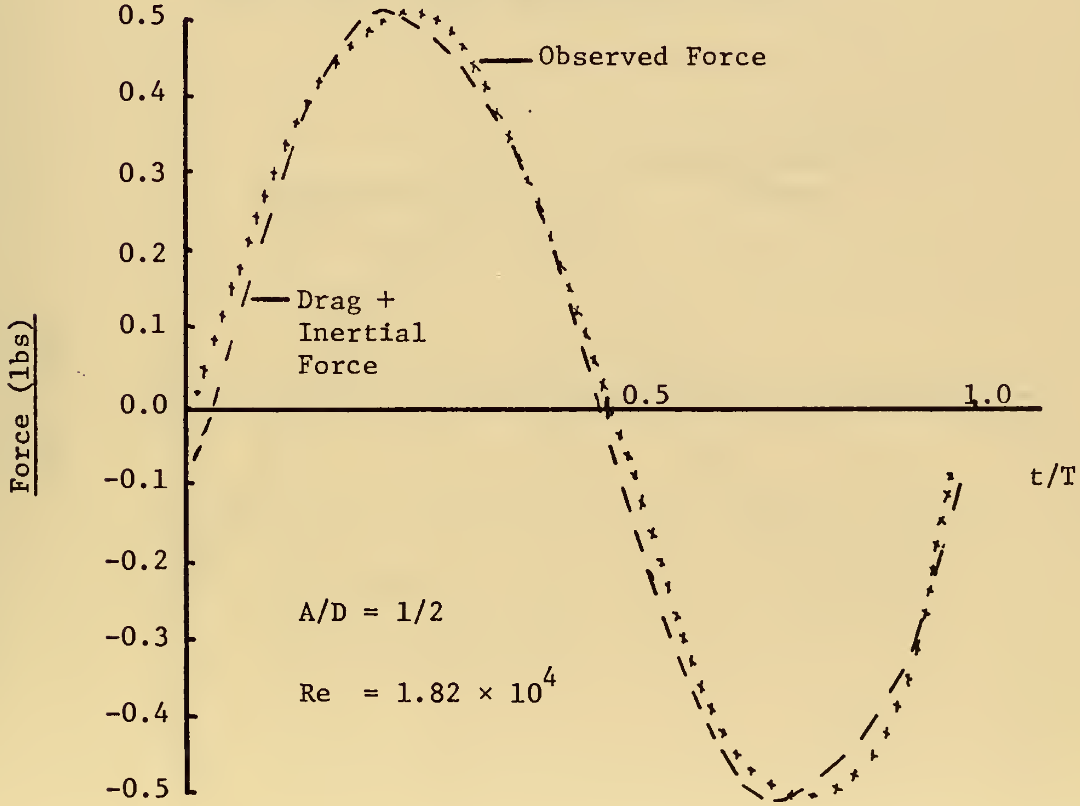

Figure 14b: Calculated vs Observed Force

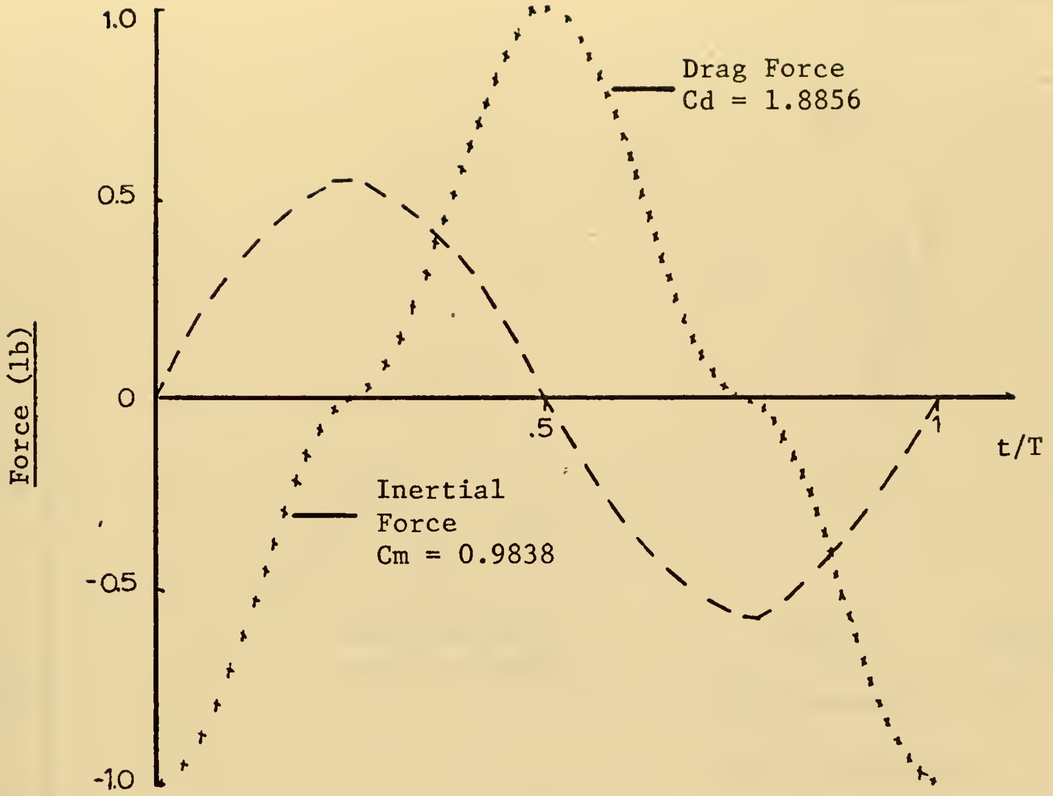

Figure 15a: Drag and Inertial Forces

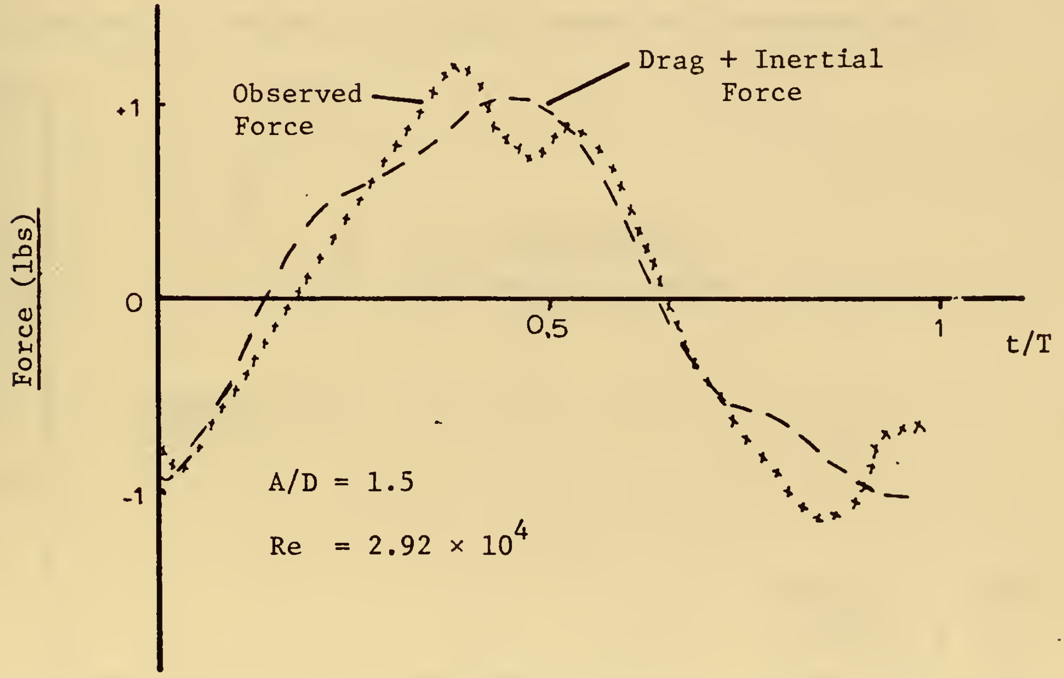

Figure 15b: Calculated vs Observed Force

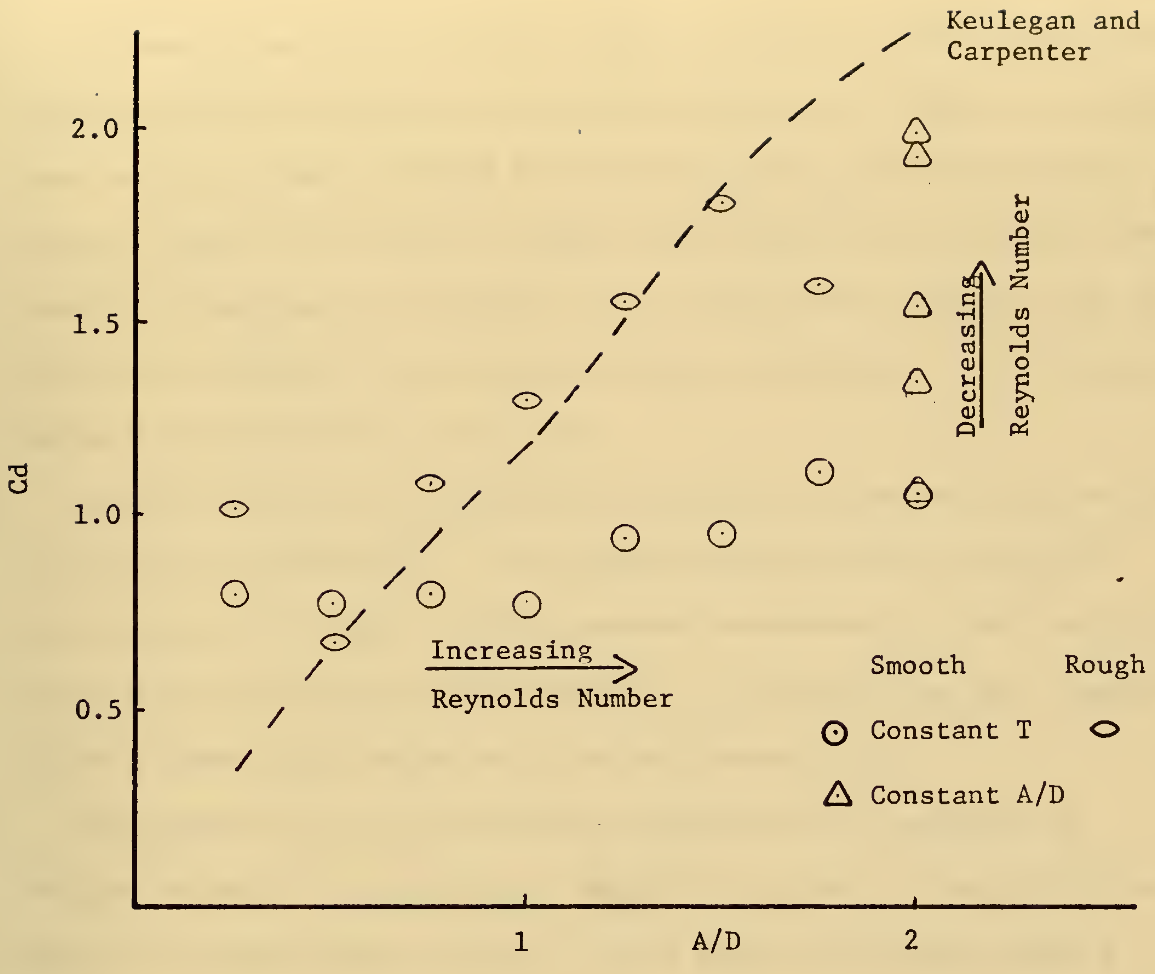

Figure 16: Effect of Reynolds Number and Roughness on Cd

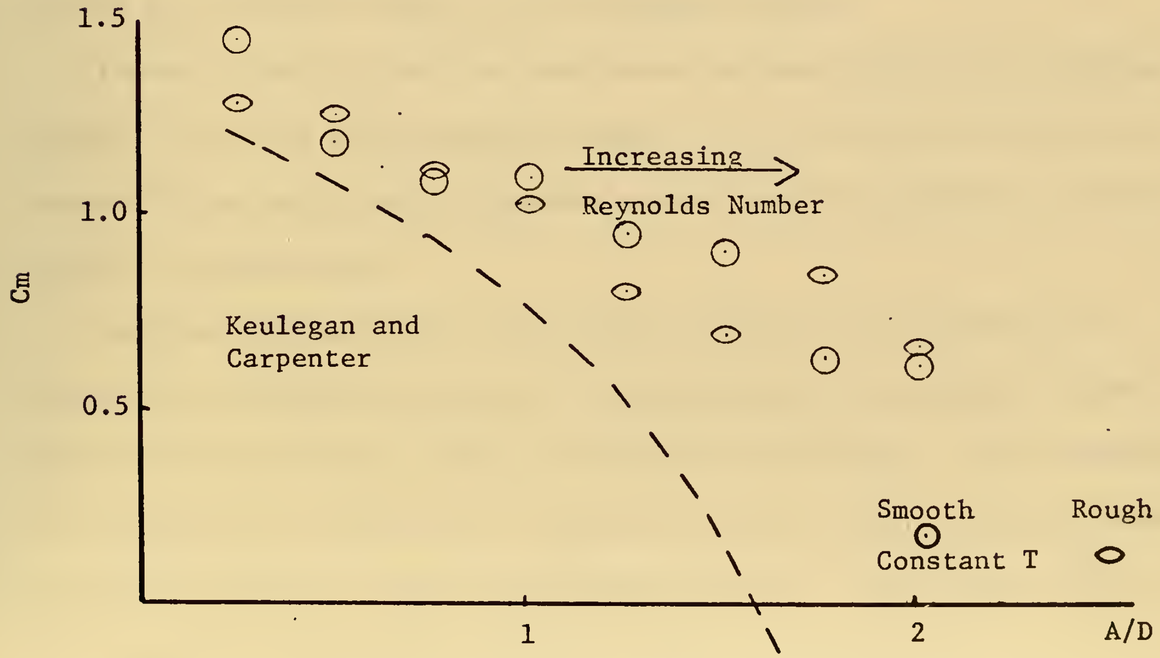

Figure 17: Effect of Reynolds Number and Roughness on Cm

It can be seen that Cd values which correspond to rather high Reynolds number, fall below Keulegan and Carpenter's results. However, the series runs which were made at fixed A/D with increasing period (decreasing Reynolds number) show that the values tend toward the low Reynolds number results of Keulegan and Carpenter. It is surprising, however, that the effect of roughness is to increase the drag coefficient so as to approach Keulegan and Carpenter's mean line.

Figure 17 shows the variation of Cm with A/D along with the results of Keulegan and Carpenter. It is noted that the results for rough cylinders and for higher Reynolds numbers encountered in this study fall above those of Keulegan and Carpenter. It is interesting that roughness tends to have little effect on Cm in the present study.

The results for Cm and Cd plotted against A/D is presented in Figures 18 and 19, respectively. No effort was made in these plots to keep the Reynolds number constant. As a result the Cd plot shows a large amount of scatter; the Cm plot, however, appears to correlate fairly well without regard for the Reynolds number.

Figure 20 and 21 show the added mass and drag coefficients plotted against A/D for a fixed Reynolds number. It is noted that the scatter caused by the non-constant Reynolds number has been suppressed, and the results correlate well.

Keulegan and Carpenter's mean lines also have been plotted for comparison on Figures 20 and 21. The magnitudes of individual points do differ but the same trends are prevalent throughout. This difference is attributed to experimental differences (particularly Reynolds number) between studies and inherent experimental error. The critical region of A/D remains in the region of 2.25 to 2.5.

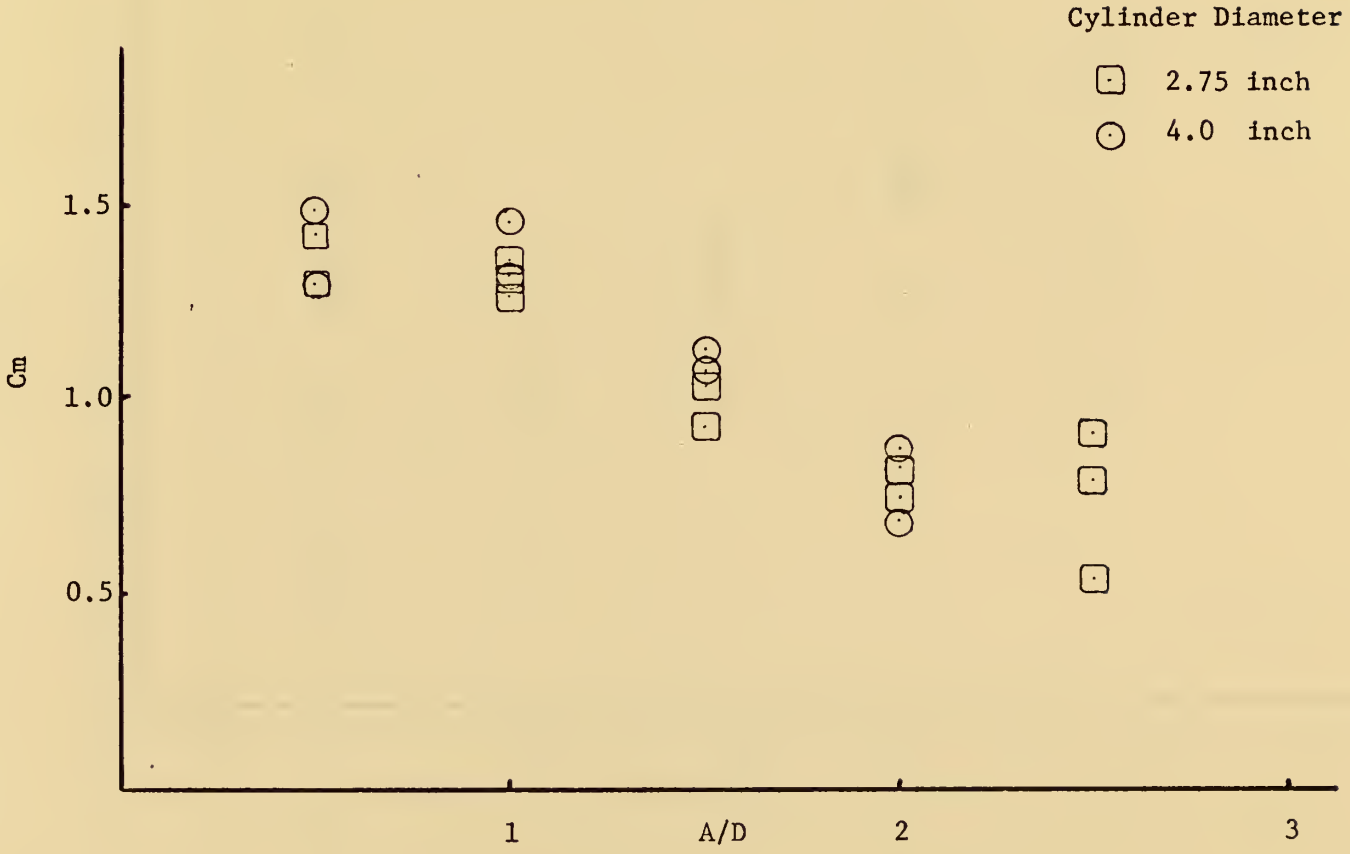

Figure 18: Inertia Coefficient - Variable Reynolds Number

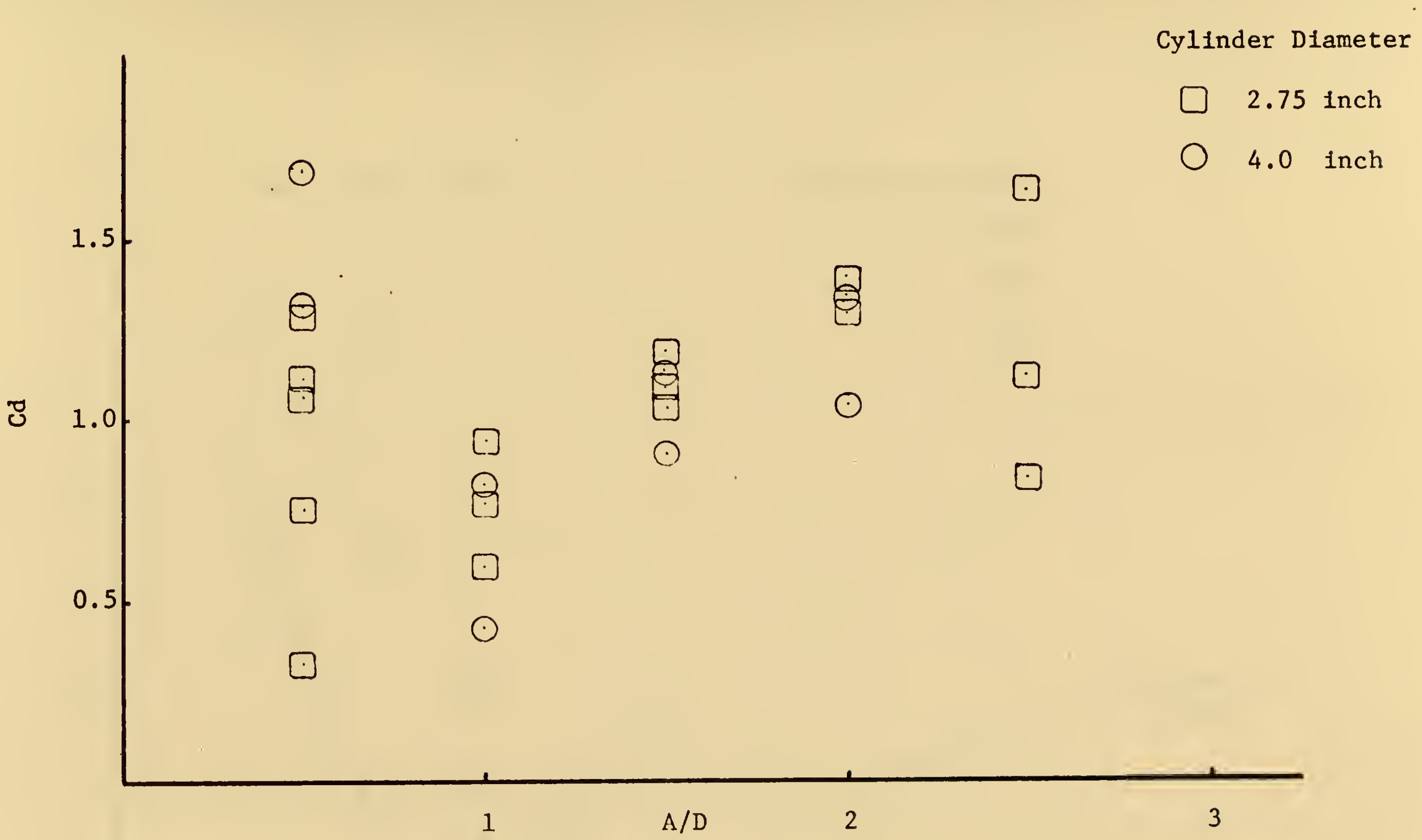

Figure 19: Drag Coefficient - Variable Reynolds Number

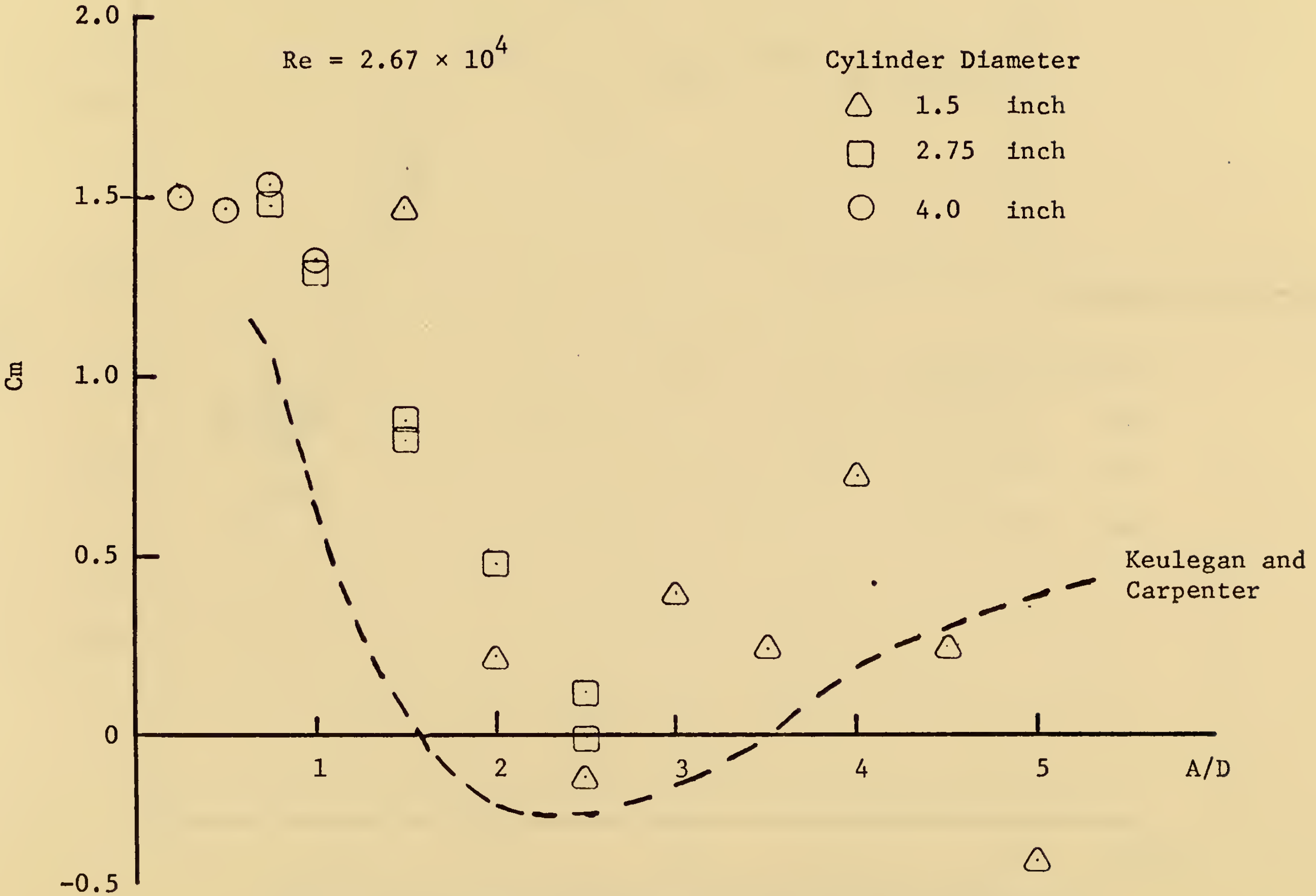

Figure 20: Inertial Coefficient, Constant Reynolds Number

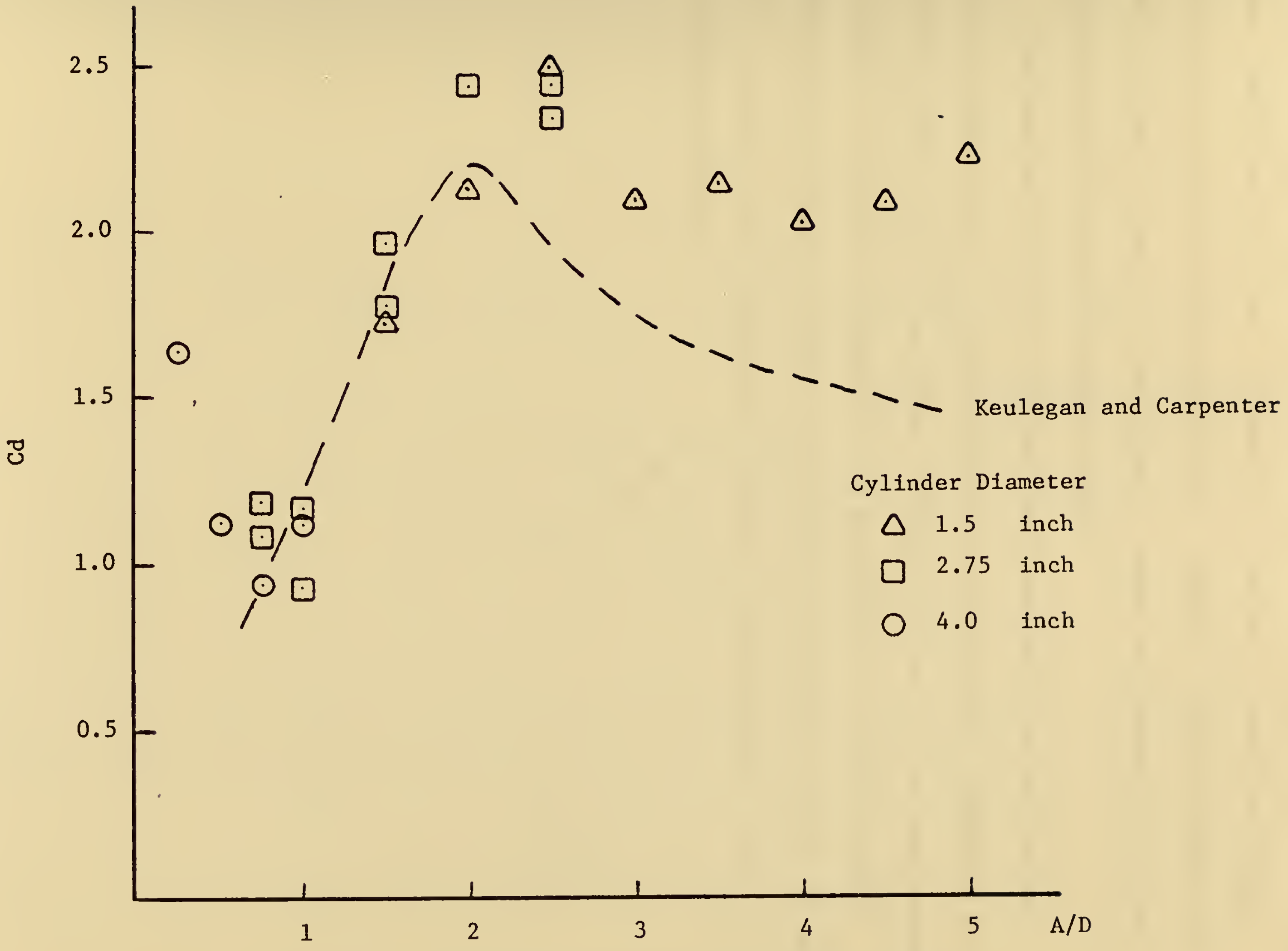

Figure 21: Drag Coefficient, Constant Reynolds Number

Figures 22 and 23 show the effect of Reynolds number on the added mass and drag coefficients, respectively. Figure 21 shows that the added mass coefficient is almost independent of Reynolds number and highly dependent upon A/D in the range tested. However, Figure 23 shows that Cd is strongly affected by the Reynolds number and generally it shows a decrease with increasing Reynolds number.

Keulegan and Carpenter [3] state that apparently no correlation exists between the two coefficients and Reynolds number. However, on plotting their data in the format of Figures 22 and 23, the same general trends are observed; Cm appears to be independent of Reynolds number while Cd is strongly dependent. This data is plotted in Figures 24 and 25. It appears that Keulegan and Carpenter overlooked this rather significant feature.

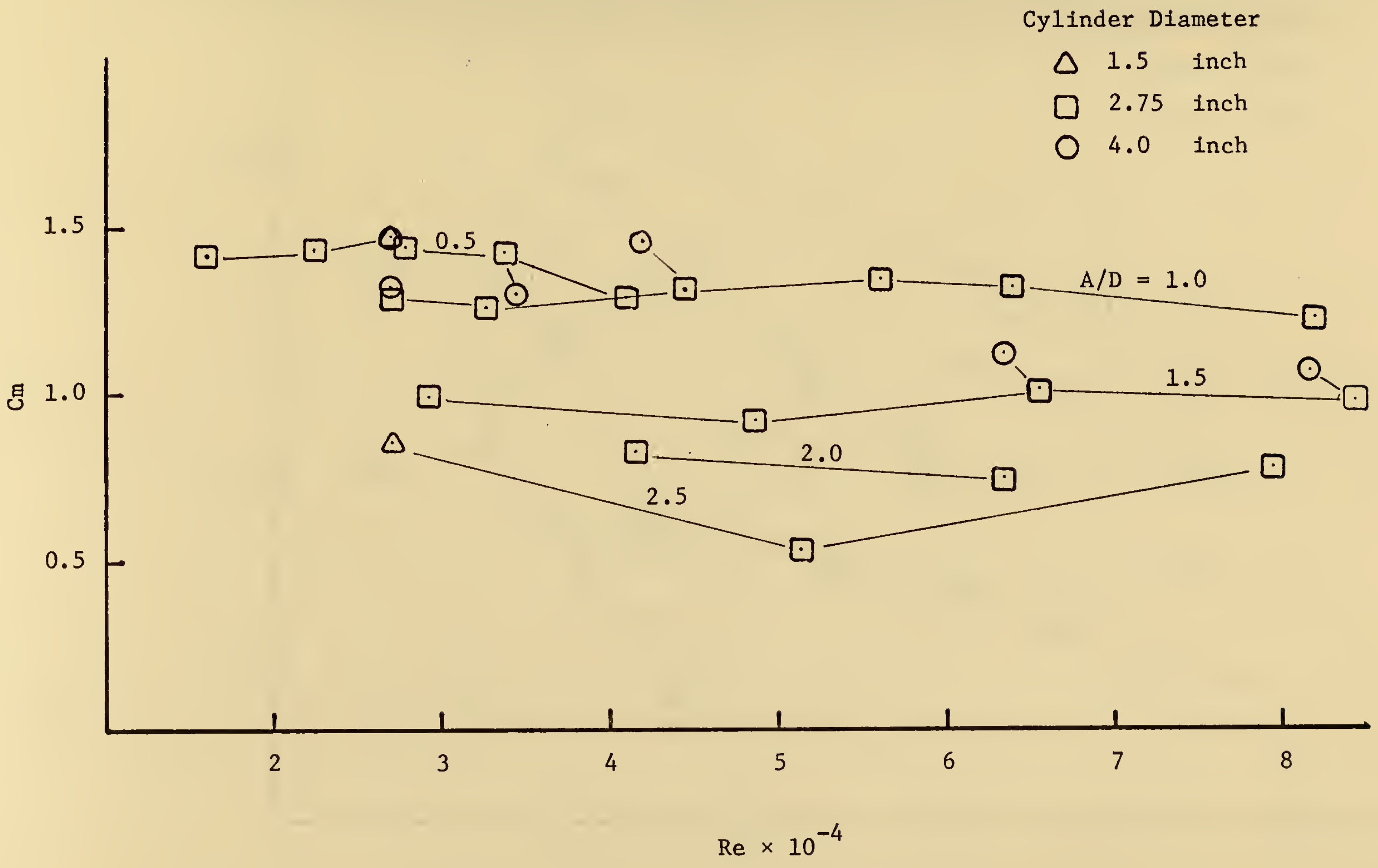

Figure 22: Effect of Reynolds Number on Cm

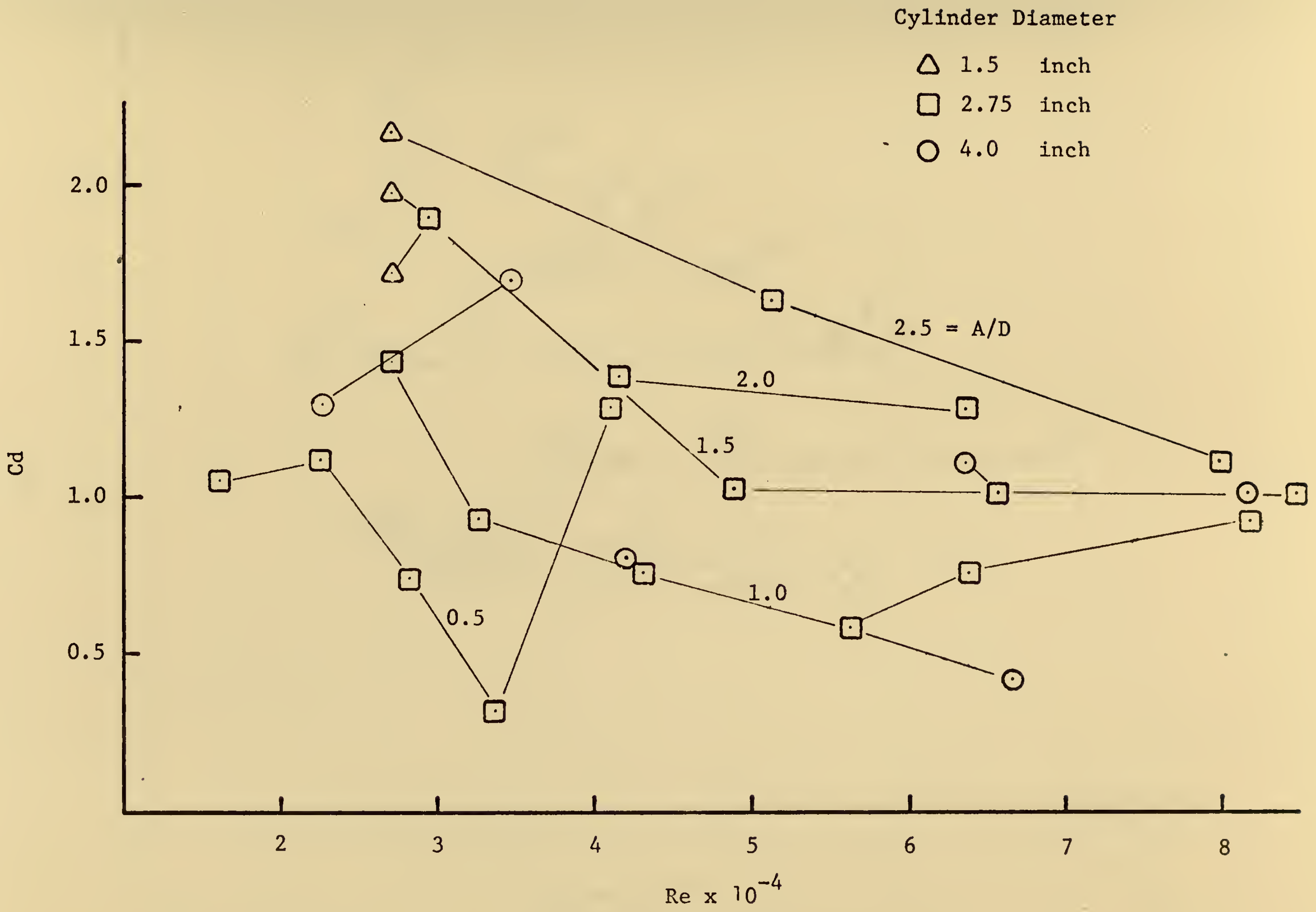

Figure 23: Effect of Reynolds Number on Cd

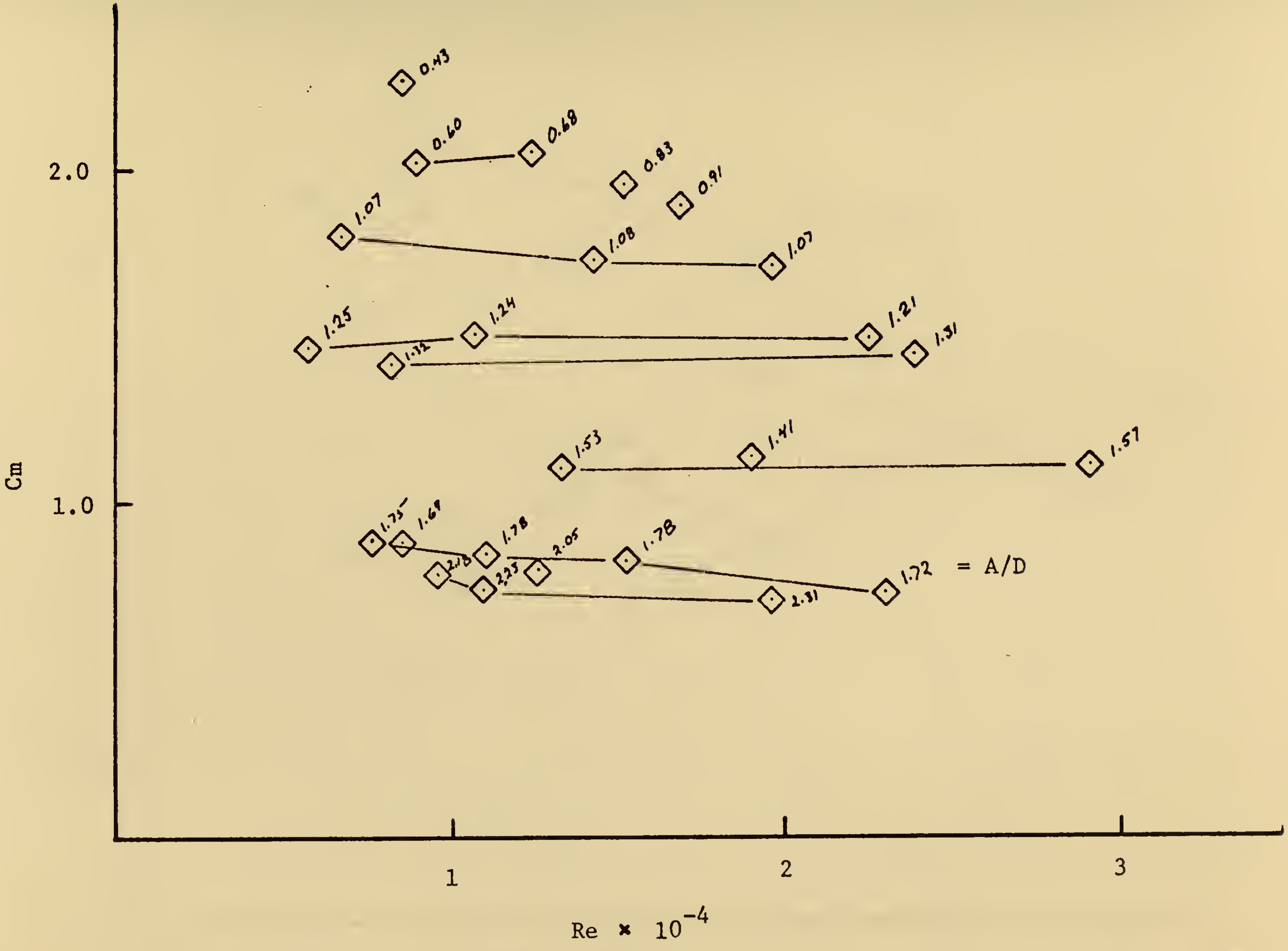

Figure 24: Keulegan and Carpenter's Data

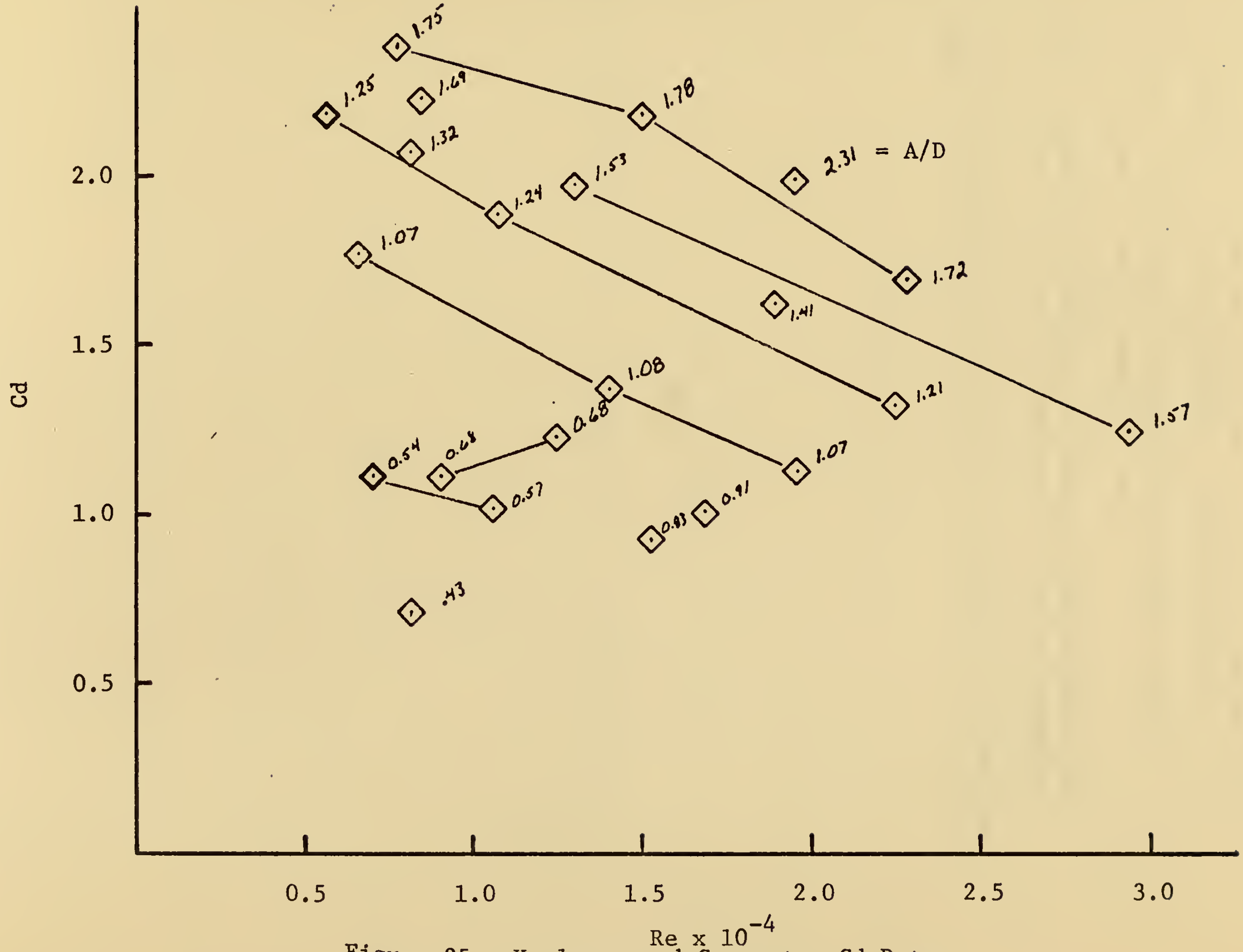

Figure 25: Keulegan and Carpenter Cd Data

VI. CONCLUSIONS

1. Total force acting on a cylinder oscillating harmonically is comprised of two components, drag and inertia.

2. The total force may be mathematically modeled using coefficients of added mass and drag.

3. Cm is primarily a function of relative displacement A/D and appears to be nearly independent of Reynolds number.

4. Cd is a function of both relative displacement and Reynolds number.

APPENDIX A

A. FORMULATION OF THE COMPUTER PROGRAM FOR DATA REDUCTION

A computer program was used to reduce the data. The purpose of the program was to compute Cm, the inertia coefficient, and Cd, the drag coefficient. The starting point for the problem was Keulegan and Carpenter's [3] formulation for these parameters. Specifically:

$$Cm = \frac{2UmT}{\pi^2 D} \int_0^{2\pi} \frac{F \sin \alpha}{\rho Um^2 D} \, d\alpha \qquad (1A)$$

and

$$Cd = -3/4 \int_0^{2\pi} \frac{F \cos \alpha}{\rho Um^2 D} \, d\alpha \qquad (2A)$$

The above integrals were transformed into the following forms:

$$Cm = \frac{2T}{\pi^3 D^2 L \rho A} \sum F \sin \left(\frac{2\pi t}{T}\right) \delta(t/T) \qquad (3A)$$

$$Cd = \frac{-3T^2}{8 \cdot \rho D\pi L A^2} \sum F \cos \left(\frac{2\pi t}{T}\right) \delta(t/T) \qquad (4A)$$

where A denotes the amplitude of the oscillatory motion and $\delta(t/T)$ was conveniently chosen as 0.05.

The corresponding error for each data set was computed by the following relationship:

$$\text{error} = \left[\frac{T^2}{2\ \rho\ D\pi^2 A^2 L} \sum F \sin \frac{6\pi t}{T}\ \delta(t/T)\right] \sin\left(\frac{6\pi t}{T}\right)$$

$$+ \left[\frac{T^2}{2\ \rho\ D\pi^2 A^2 L} \sum F \cos\left(\frac{6\pi t}{T}\right) \delta(t/T)\right.$$

$$\left. - 0.02 \sum F \cos\left(\frac{6\pi t}{T}\right) \delta(t/T)\right] \cos\,(6\pi\ t/T) \tag{5A}$$

where:

T = period in seconds

D = cylinder diameter in feet

L = cylinder diameter in feet

t = time

This error function is obtained by subtracting the computed values from the observed.

The program employed time increments of 1/20 T. where t/T takes on values from zero to one. For each run at constant period it was possible to fix t/T increments for each data set.

B. FLOW CHART OF COMPUTER PROGRAM

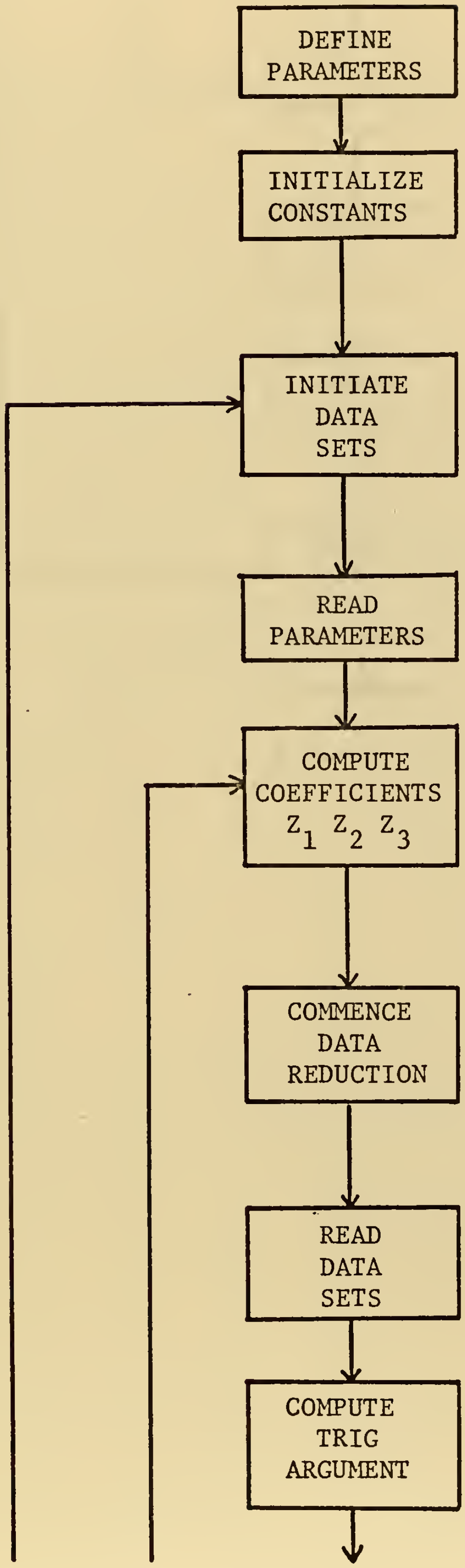

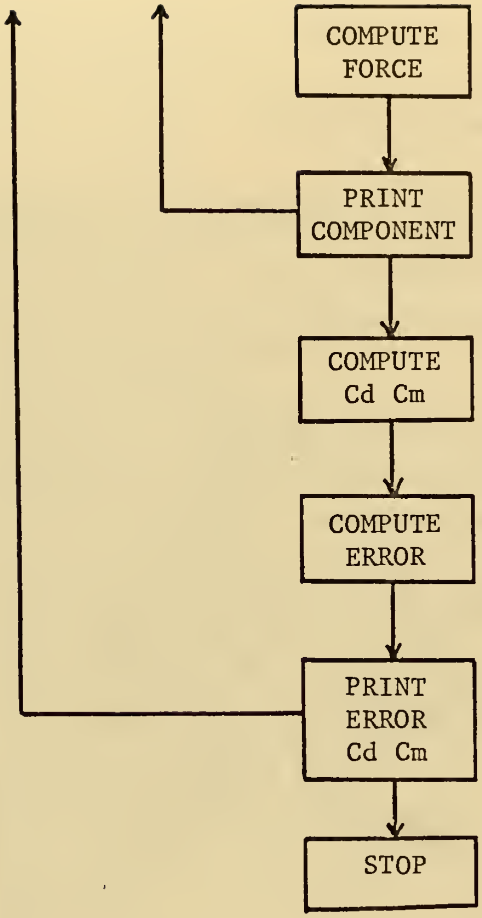
COMPUTE FORCE
PRINT COMPONENT
COMPUTE Cd Cm
COMPUTE ERROR
PRINT ERROR Cd Cm
STOP

APPENDIX B

COMPUTER PROGRAM

```
   10 FORMAT(3F10.4,I10)
   15 FORMAT('1',10X,'DIA=',F8.4,5X,'AMP=',F8.4,5X,'PER=',F8
     1.4,5X,'Z1='
     1F8.4,5X,'Z2=',F8.4,5X,'Z3=',F8.4,5X,'NCARD=',I3)
     1',8X,'F',11X
   20 FORMAT('0',3X,'TIME/PER',7X,'ALPHA',7X,'COSA',8X,'SINA
     1,'FCOSA',8X,'FSINA')
   25 FORMAT(2F10.4)
   30 FORMAT('0',7F12.4)
   35 FORMAT('0',7X,'CM=',7X,'CD=',7X,'BETA=')
   40 FORMAT('0',3F12.4)
   45 FORMAT('0',10X,'A3=',F8.4,5X,'B1=',F8.4,5X,'B3=',F8.4,
     15X,'B3P=',F8.4)
   50 FORMAT('0',3X,'TIME/PER',7X,'ALPHA',7X,'SIN3A',7X,'COS
     13A',7X,'ERROR')
   55 FORMAT('0',5F12.4)
C     TIME=DIMENSIONLESS TIME (TIME/PERIOD)
C     BETA=DIMENSIONLESS DISPLACEMENT (UMAX*PER/DIA)
C     L=CYLINDER LENGTH IN FEET
C     DIA=DIAMETER OF CYLINDER IN FEET
C     AMP=AMPLITUDE OF MOTION IN FEET
C     PER=PERIOD IN SECS (CHART PERIOD/CHART SPEED)
C     ZI=FORCE COEFFICIENTS
C     CM=INERTIA COEFFICIENT
C     CD=DRAG COEFFICIENT
C     ERROR=REMAINDER FUNCTION
C     A1,BI=FOURIER COEFFICIENTS
C     K=CONSTANT
C     N=NUMBER OF DATA SETS
      G=32.174
      RHO=62.4/G
      K=0.2
      PI=3.14159
      L=1.375
C     INITIATE DATA SETS
      N=9
      DO 100 I=1,N
      A3=0.0
      B1=0.0
      B3=0.0
      CM=0.0
      CD=0.0
C     READ IN PARAMETERS WHICH CHARACTERIZE THE DATA SET
      READ(5,10) DIA,AMP,PER,NCARD
C     COMPUTE FORCE COEFFICIENTS
      Z1=2*PER**2/(PI**3*DIA**2*L*RHO*AMP)
      Z2=-3*PER**2/(8*RHO*DIA*PI*L*AMP**2)
      Z3=PER**2/(2*RHO*DIA*PI**2*AMP**2*L)
C     COMPUTE BETA
      BETA=2*PI*AMP/DIA
C     PRINT OUT PARAMETERS AND COEFFICIENTS
      WRITE(6,15) DIA,AMP,PER,Z1,Z2,Z3,NCARD
C     PRINT OUT FORMAT
      WRITE(6,20)
C     COMMENCE DATA REDUCTION
      DO 1000 J=1,NCARD
      READ(5,25) TIME,F
      ALPHA=2*PI*TIME
      SINA=SIN(ALPHA)
      SIN3A=SIN(3*ALPHA)
      COSA=COS(ALPHA)
      COS3A=COS(3*ALPHA)
      FSINA=0.05*F*SINA
```

```
      FSIN3A=0.05*F*SIN3A
      FCOSA=0.05*F*COSA
      FCOS3A=0.05*F*COS3A
C     SUM COMPONENTS
      CM=FSINA+CM
      CD=FCOSA+CD
      A3=FSIN3A+A3
      B1=FCOSA+B1
      B3=FCOS3A+B3
C      PRINT OUT COMPONENTS FOR DRAG AND INERTIA COEFFICIENT
      WRITE(6,30) TIME,ALPHA,COSA,SINA,F,FCOSA,FSINA
 1000 CONTINUE
C      COMPUTE COEFFICIENTS
      CM=Z1*CM
      CD=Z2*CD
      A3=Z3*A3
      B1=Z3*B1
      B3P=Z3*B3-K*B1
C     PRINT OUT INERTIA AND DRAG COEFFICIENTS
      WRITE(6,35)
      WRITE(6,40) CM,CD,BETA
C     COMPUTE ERROR
C     PRINT OUT ERROR FORMAT
      WRITE(6,45) A3,B1,B3,B3P
      WRITE(6,50)
      TIME=0.025
      DO 1500 K=1,NCARD
      ALPHA=2*PI*TIME
      SIN3A=SIN(3*ALPHA)
      COS3A=COS(3*ALPHA)
      ERROR=A3*SIN3A+B3P*COS3A
C     PRINT OUT ERROR COMPONENTS AND ERROR
      WRITE(6,55) TIME,ALPHA,SIN3A,COS3A,ERROR
      TIME=TIME+0.05
 1500 CONTINUE
  100 CONTINUE
      STOP
      END
```

APPENDIX C

A. CALCULATION OF INERTIAL AND DRAG FORCES

Given

$$T, \ Cd, \ Cm, \ D, \ Am, \quad \text{and}$$

$$\rho = 1.93 \text{ slugs}$$

$$F = F_I + F_D = Cm \ \rho \ Ao \frac{dU}{dt} + \frac{1}{2} Cd \ D \ \rho \ U \ |U|$$

$$F_I = Cm \ \rho \ Ao \frac{dU}{dt} = Cm \frac{\rho \pi D^2}{4} \frac{dU}{dt}$$

$$U = -Um \cos \sigma t \qquad \frac{dU}{dt} = Um \ \sigma \sin \sigma t$$

$$\sigma = 2 \pi / T$$

$$Um = 2 \pi \frac{Am}{T}$$

Therefore:

$$\frac{dU}{dt} = \frac{2\pi \ Am}{T} \frac{2\pi}{T} \sin \sigma t$$

$$= \frac{4\pi^2 \ Am}{T^2} \sin \sigma t$$

Therefore:

$$F_I = Cm \frac{\rho\pi \ D^2}{4} \frac{4\pi^2 \ Am}{T^2} \sin \frac{2\pi t}{T}$$

Let $$\alpha = \frac{2\pi t}{T} = \alpha(t)$$

with $$\alpha = 2\pi \quad t/T$$

$$F_I = \frac{Cm\ \rho\ \pi^3\ D^2\ Am}{T^2} \sin\alpha$$

$$F_D = \frac{1}{2} Cd\ D\ \rho\ U\ |U|$$

substituting for U

$$F_D = -\frac{1}{2} Cd\ D\ \rho\ Um^2\ |\cos\sigma t|\cos\sigma t$$

substituting for Um

$$F_D = -\frac{1}{2} Cd\ D\ \rho\ \frac{4\pi^2\ Am^2}{T^2} \cos\sigma t\ |\cos\sigma t|$$

therefore

$$F_D = -Cd\ \frac{2D\ \rho\ \pi^2\ Am^2}{T^2} \cos\alpha\ |\cos\alpha|$$

when α is substituted for σt.

CALCULATED DRAG AND INERTIA FORCE FOR:

$T = 1.60$ seconds $C_m = 1.1722$ $C_d = 0.7947$

$\rho = 1.93$ slugs $A = 0.1667$ ft. $D = 0.3333$ ft.

$$F_I = 0.508 \sin \alpha$$

$$F_D = -0.110 \cos \alpha \left| \cos \alpha \right|$$

$$F_C = F_I + F_D$$

Time Period	Inertial Force	Drag Force	Calculated Force	Observed Force
0.25	0.079	-0.107	-0.027	0.05
0.75	0.230	-0.087	0.143	0.20
1.25	0.360	-0.055	0.304	0.33
1.75	0.453	-0.023	0.430	0.43
2.25	0.502	-0.003	0.499	0.50
2.75	0.507	0.003	0.505	0.50
3.25	0.453	0.023	0.475	0.50
3.75	0.360	0.550	0.414	0.45
4.25	0.230	0.087	0.318	0.35
4.75	0.080	0.107	0.187	0.17
5.25	-0.080	0.107	0.048	0.05
5.75	-0.230	0.087	-0.143	-0.10
6.25	-0.360	0.055	-0.304	-0.25
6.75	-0.453	0.023	-0.430	-0.40
7.25	-0.502	0.003	-0.499	-0.45
7.75	-0.502	-0.003	-0.505	-0.50
8.25	-0.453	-0.023	-0.475	-0.50
8.75	-0.360	-0.055	-0.414	-0.45
9.25	-0.230	-0.087	-0.318	-0.35
9.75	-0.079	-0.107	-0.187	-0.10

CALCULATED DRAG AND INERTIA FORCES FOR:

T = 1.39 seconds　　Cm = 0.9838　　Cd = 1.8856

ρ = 1.93 slugs　　Am = 0.3437 ft.　　D = 0.2991 ft.

$F_I = 0.667 \sin \alpha$

$F_D = -3.17 \cos \alpha \,|\cos \alpha|$

$F_C = F_I + F_D$

Time Period	Inertial Force	Drag Force	Calculated Force	Observed Force
0.025	0.087	-0.983	-0.896	-0.900
0.075	0.252	-0.800	-0.548	-0.600
0.125	0.393	-0.504	-0.111	-0.300
0.175	0.496	-0.207	0.289	0.000
0.225	0.550	-0.024	0.525	0.300
0.275	0.550	0.024	0.574	0.600
0.325	0.496	0.207	0.703	0.900
0.375	0.393	0.504	0.897	1.200
0.425	0.252	0.800	1.052	0.900
0.475	0.087	0.983	1.070	0.700
0.525	-0.087	0.983	0.896	0.900
0.575	-0.252	0.800	0.548	0.700
0.625	-0.393	0.504	0.111	0.250
0.675	-0.496	0.207	-0.289	-0.250
0.725	-0.550	0.024	-0.525	-0.600
0.775	-0.550	-0.024	-0.574	-0.800
0.825	-0.496	-0.207	-0.703	-1.100
0.875	-0.393	-0.504	-0.897	-1.100
0.925	-0.252	-0.800	-1.052	-0.700
09.75	-0.087	-0.983	-1.070	-0.650

APPENDIX D

DATA RUNS FOR REYNOLDS NUMBER 2.7×10^4

Runs	Cyl. Dia.	A/D	T	Cm	Cd
R1	1.5 in.	1.5	0.46	1.4692	1.7197
R2	1.5	2.0	0.60	0.2134	2.1625
R3	1.5	2.5	0.78	-0.1047	2.4826
R4	1.5	3.0	0.91	0.3988	2.0726
R5	1.5	3.5	1.05	0.2462	2.1140
R6	1.5	4.0	1.21	0.7225	2.0300
R7	1.5	4.5	1.37	0.0249	2.0825
R8	1.5	5.0	1.56	-0.3539	2.2148
R9	2.75	0.75	0.75	1.4791	1.1915
R10	2.75	0.75	0.75	1.4594	1.0918
R11	2.75	1.0	1.0	1.2939	1.1664
R12	2.75	1.0	0.96	1.2832	0.9221
R13	2.75	1.5	1.50	0.8159	1.7550
R14	2.75	1.5	1.45	0.8762	1.9681
R15	2.75	2.0	2.06	-0.6060	2.9893
R16	2.75	2.5	2.53	0.1127	2.3252
R17	2.75	2.5	2.57	-0.0085	2.4444
R18	4.0	1/4	0.53	1.4959	1.6421
R19	4.0	3/4	1.50	1.5350	0.9485
R20	4.0	1/2	1.06	1.4632	1.1187
R21	4.0	1.0	2.15	1.3128	1.1295

DATA RUNS FOR VARIABLE REYNOLDS NUMBER

Run	A/D	T	Cm	Cd	Re × 10^{-4}
1.	1/2	0.84	1.4201	1.0556	1.61
2.	1/2	0.60	1.4358	1.1032	2.25
3.	1/2	0.48	1.4395	0.7405	2.82
4.	1/2	0.40	1.4244	0.3118	3.38
5.	1/2	0.33	1.2812	1.2897	4.10
6.	1	0.83	1.2561	0.9318	3.26
7.	1	0.61	1.3029	0.7524	4.43
8.	1	0.48	1.3375	0.5872	5.63
9.	1	0.39	1.3154	0.7546	6.39
10.	1	0.33	1.2295	0.9274	8.19
11.	1.5	1.39	0.9838	1.8856	2.92
12.	1.5	0.83	0.9190	1.1842	4.89
13.	1.5	0.62	1.0179	1.0826	6.54
14.	1.5	0.48	0.9710	1.0334	8.45
15.	2	1.30	0.8083	1.3861	4.16
16.	2	0.85	0.7454	1.2833	6.36
17.	2.5	1.32	0.5224	1.6231	5.12
18.	2.5	0.85	0.7891	1.1180	7.95
19.	2.5	0.55	0.9003	0.8348	12.30
20.	1/2	1.26	1.4857	1.2957	2.26
21.	1/2	0.83	1.2976	1.6856	3.43
22.	1	1.36	1.4547	0.8183	4.20
23.	1	0.86	1.3394	0.8546	6.64
24.	1.5	1.35	1.1263	1.1111	6.35
25.	1.5	1.05	1.0685	1.0063	8.17
26.	1.5	0.84	1.1361	0.8950	10.10

Runs 1 - 19	2.75 inch diameter cylinder
Runs 20 - 26	4.00 inch diameter cylinder

BIBLIOGRAPHY

1. Reid, R. O. and Bretschneider, C. L., "The Design Wave in Deep and Shallow Water and Forces on Pilings and Large Submerged Objects", A. and M. College of Texas, Dept. of Oceanography, Tech Report on Contract NOy 27474, DA - 49 - 005 - eng - 18, and N7 onr - 48704, 36 pp., February 1954 (unpublished).

2. Weigel, R. L., "Oceanographical Engineering", Prentice - Hall, 1964.

3. Keulegan, G. H., and Carpenter, L. H., "Forces on Cylinders and Plates in an Oscillating Fluid", Journal of Research of the National Bureau of Standards, v. 60, no. 5, p. 423-440, May 1958.

4. Heinzer, A. J., "Experimental Investigation of the Wake of an Oscillating Cylinder", Unpublished Master's Thesis, University of Houston, Houston, Texas, 1968.

5. Sarpkaya, T., and Garrison, C. J., "Vortex Formation and Resistance in Unsteady Flow", Journal of Applied Mechanics Transactions of the ASME, v. 30, series E, no. 1, p. 16-24, March 1963.

6. Morison, J. R., O'Brien, M. P., Johnson, J. W., and Schaaf, S. A., "The Force Exerted by Surface Waves on Piles", Journal of Petroleum Technology, American Institute of Mining and Metallurgical Engineers, v. 189, p. 149-154, May 1950.

7. McNown, J. S., and Wolf, L. W., "Resistance to Unsteady Flow: I. Analysis of Tests with Flat Plate", Engineering Research Institute of Michigan, 2446 - I - P, June 1956. Internal report to Sandia Corporation.

INITIAL DISTRIBUTION LIST

		No. Copies
1.	Defense Documentation Center Cameron Station Alexandria, Virginia 22314	2
2.	Library, Code 0212 Naval Postgraduate School Monterey, California 93940	2
3.	Asst. Professor C. J. Garrison Code 59Gm Department of Mechanical Engineering Naval Postgraduate School Monterey, California 93940	3
4.	Professor T. Sarpkaya Code 59Si Department of Mechanical Engineering Naval Postgraduate School Monterey, California 93940	1
5.	Lt. John R. Driscoll, Jr. USN 877 Crestline Drive Blue Bell, Pennsylvania 19422	2
6.	Department of Mechanical Engineering Library, Code 59 Naval Postgraduate School Monterey, California 93940	1

UNCLASSIFIED
Security Classification

DOCUMENT CONTROL DATA - R & D

(Security classification of title, body of abstract and indexing annotation must be entered when the overall report is classified)

ORIGINATING ACTIVITY *(Corporate author)* Naval Postgraduate School Monterey, California 93940	2a. REPORT SECURITY CLASSIFICATION Unclassified
	2b. GROUP

REPORT TITLE

Forces on Cylinders Oscillating in Water

DESCRIPTIVE NOTES *(Type of report and, inclusive dates)*

Master's Thesis; December 1972

AUTHOR(S) *(First name, middle initial, last name)*

John R. Driscoll, Jr.

REPORT DATE December 1972	7a. TOTAL NO. OF PAGES 63	7b. NO. OF REFS 7
8a. CONTRACT OR GRANT NO.	9a. ORIGINATOR'S REPORT NUMBER(S)	
b. PROJECT NO.		
c.	9b. OTHER REPORT NO(S) *(Any other numbers that may be assigned this report)*	
d.		

10. DISTRIBUTION STATEMENT

Approved for public release; distribution unlimited.

11. SUPPLEMENTARY NOTES	12. SPONSORING MILITARY ACTIVITY Naval Postgraduate School Monterey, California 93940

13. ABSTRACT

A circular cylinder immersed in an infinite fluid and oscillated perpendicular to its axis is acted upon by a fluid dynamic force. This force is generally considered to be composed of two components, a drag and an added mass component. The relative importance of these are functions of the frequency and displacement of the cylinder.

It was the purpose of this study to determine experimentally these two components as a function of the ratio of the displacement amplitude to the cylinder diameter, and the Reynolds number based on the maximum velocity.

DD FORM 1 NOV 65 1473 (PAGE 1)

S/N 0101-807-6811

UNCLASSIFIED
Security Classification

A-31408

14. KEY WORDS	LINK A		LINK B		LINK C	
	ROLE	WT	ROLE	WT	ROLE	WT
UNSTEADY FLOW DRAG ADDED MASS						

DD FORM 1 NOV 65 1473 (BACK)
S/N 0101-807-6821

A-31409

141466
Thesis
D753 Driscoll
c.1 Forces on cylinders
oscillating in water.